Westinghouse Non-Proprietary Class 3

WCAP-16766-NP October 2007

Westinghouse Next Generation Correlation (WNG-1) for Predicting Critical Heat Flux in Rod Bundles with Split Vane Mixing Grids

Westinghouse

WCAP-16766-NP

Westinghouse Next Generation Correlation (WNG-1) for Predicting Critical Heat Flux in Rod Bundles with Split Vane Mixing Grids

October 2007

Authors:

P. F. Joffre
Y. Sung
R. Mathur
L. D. Smith, III
P. A. Hilton

Prepared by:
W. Slagle*

Approved by:
R. Sisk*

* Electronically Approved Records Are Authenticated in the Electronic Document Management System

Westinghouse Electric Company LLC
4350 Northern Pike
Monroeville, PA 15146

Page Intentionally Left Blank

Abstract

This report describes the development of Westinghouse Next Generation Critical Heat Flux (CHF) correlation (WNG-1) for Pressurized Water Reactor (PWR) fuel designs containing structural mixing vane (MV) grids and Intermediate Flow Mixer (IFM) grids with split vanes. The WNG-1 correlation was developed for the Westinghouse Next Generation Fuel, but can be used for current fuel designs containing split vane grids that are enveloped by the database. The WNG-1 correlation coefficients were derived with the Westinghouse version of the VIPRE-01 (VIPRE) subchannel code. The correlation was developed based on CHF test data obtained from the Heat Transfer Research facility of Columbia University. The tests simulated 4x4, 5x5 and 6x6 arrays of the fuel assembly geometry, split vane mixing grids, uniform and non-uniform axial power shapes, non-uniform radial power distributions, with and without guide thimbles, varied heated lengths and grid spacing. The functional form of the CHF correlation is empirical and is based solely on experimental observations of the relationship between the measured CHF and the correlation variables. The same correlation form has been previously used for other PWR fuel designs. The correlation includes the following variables: pressure, local mass velocity, local quality, a grid spacing term (GST), heated length from inlet to CHF location and the heated hydraulic diameter ratio of the CHF channel. The grid spacing term, GST, is defined as the [ ] a, c. The heated hydraulic diameter ratio is defined as the [ ] a, c. Special geometry terms are applied to the correlation to account for grid spacing, heated length, and cold wall effects. Based upon the uniform and non-uniform data [ ] a, c, an optimized non-uniform shape factor, F_C, is developed for the split vane mixing grid geometries covered by the correlation. The 95/95 DNBR limit for the WNG-1 CHF correlation is 1.14. The WNG-1 correlation will be used with Westinghouse version of the VIPRE code. The range of applicability for the WNG-1 correlations is summarized as follows:

Parameter	**WNG-1 Correlation Parameter Range**
Pressure (psia)	1405 to 2495
Local mass velocity (Mlbm/hr-ft^2)	0.79 to 3.72
Local quality (fraction)	≤ 0.43
Heated length, inlet to CHF location (inches)	48* to 168
Grid spacing (inches)	6.4 to 26
Heated hydraulic diameter ratio, [ ] a, c	0.85 to 1.00
Matrix Heated Hydraulic Diameter, Dhm (inches)	0.46 to 0.53
Grid Spacing Term, GST [ ] a, c	≥ 26.5

* Set as Minimum HL value, applied at all elevations below 48 inches

Page Intentionally Left Blank

Table of Contents

List of Tables

List of Figures

Page Intentionally Left Blank

1.0 Introduction

This report describes the development of the Westinghouse Next Generation Critical Heat Flux (CHF) correlation (WNG-1) for Pressurized Water Reactor (PWR) fuel designs containing structural mixing vane (MV) grids and Intermediate Flow Mixer (IFM) grids. A CHF correlation is also commonly referred to as a Departure from Nucleate Boiling (DNB) correlation. The WNG-1 correlation was developed for the Westinghouse Next Generation Fuel, but can be used for current designs containing split vane grids that are enveloped by the database. The split vane designs, included in the WNG-1 correlation database, are illustrated in Figure 1-1. The WNG-1 correlation form is essentially the same as the WSSV and WSSV-T correlations for Combustion Engineering PWR (CEPWR) fuel designs containing grids with side-supported vanes, Reference 1. Adjustments to the correlation form are due to the differences in the grid mixing vane design and the thimble tube geometry. The correlation coefficients were derived with Westinghouse version of the VIPRE-01 (VIPRE) subchannel code, Reference 2.

This correlation was developed based on Westinghouse Critical Heat Flux (CHF) test data obtained from the Heat Transfer Research Facility of Columbia University. The test data used in the correlation development and validation are from 4x4, 5x5 and 6x6 rod bundles simulating the Westinghouse PWR (W-PWR) fuel designs. The Westinghouse Next Generation Fuel (NGF) 17x17 design may contain 2 IFM grids located consecutively in a grid span between two MV grids. To provide sufficient data to cover different grid spacings, the WNG-1 database also contains previous CHF tests for existing fuel designs. Tests were performed with uniform and non-uniform axial power shapes for test arrays with and without guide thimbles. The test sections have heated lengths ranging from 96 inches to 168 inches, grid spacing of 6.4 inches to 26 inches, and rod diameter ranging from 0.360 inches to 0.423 inches.

The following sections describe why the new correlation was developed and a brief summary of the contents of the report.

1.1 Need for New Correlation

The WNG-1 correlation was developed for the following reasons:

1) A new correlation is needed to accurately reflect thermal performance of the Next Generation Fuel (NGF) designs with the split vane grids. The NGF design may have up to three grid span values over the length of the bundle. For example, for the 17x17 NGF 5-IFM design with a nominal heated length of 12 feet, the lower region has 20.55 inch grid spacing, the center region has 10.28 inch grid spacing and the upper region has grid spacing as low as 6.4 inches.
2) The new correlation should be applicable to a wider parameter range than the existing correlation (e.g., local quality higher than 30%), in support of extended power uprate.

Westinghouse has developed several new fuel designs, collectively identified as the Next Generation Fuel Design in 16x16 and 17x17 lattices. [ ] [a,c] shown in Figure 1-1 are covered by the WNG-1 correlation database. For the NGF designs, grid spacing varies depending on number of IFM grids in a grid span. A new DNB correlation is needed to accurately reflect thermal margin of the NGF design.

To develop a correlation for these designs, CHF test data were taken with the NGF grid and fuel designs at the Heat Transfer Research Facility of Columbia University. Since the correlation needed to cover a large range of grid spacing, mixing grid data from previous testing were included in the development of the final correlation form and constants to make the correlation robust and to cover the W-PWR fuel designs with the 0.422 inch rod diameter. The database also included the data for the 17x17 Robust Fuel Assembly (RFA) design, Reference 3, and the data for the 17x17 and 16x16 designs in Europe as documented in Reference 4. All of those fuel designs use grids with split vanes.

Both uniform and non-uniform axial power data were included in the database for the WNG-1 correlation. This provided the data required to develop an optimized non-uniform shape factor, F_C, for the correlation. The data at the measured elevation [

] [a,c] the single tube and annular geometry used in the development of the Tong non-uniform shape factor, Reference 5. The data at the measured elevation were then used to optimize the non-uniform shape factor for the split vane data with small thimble tubes.

The WNG-1 correlation has been developed primarily for application for the new NGF fuel designs. The WNG-1 correlation also has a wider parameter range than an existing DNB correlation for fuel designs covered by its database. Since the correlation is developed with multiple fuel designs, it is considered to be applicable for the designs that fall within the parameter range. The WNG-1 correlation is considered to be applicable to the following designs:

- W-PWR Next Generation Fuel (NGF) or Upgrade designs with 0.360, 0.374 and 0.422-inch diameter rods and split vane mid-grid designs.
- Westinghouse 17x17 Robust Fuel Assembly (RFA) designs at high quality and/or low flow (outside the range of the WRB-2M correlation, Reference 3).

However, the WNG-1 correlation does not supersede any existing correlations, Reference 3, 6 or 7, applied for the current fuel designs.

1.2 The WNG-1 PWR CHF Correlation

Similar to the WSSV correlation for the CE-PWR NGF fuel design, Reference 1, the WNG-1 correlation is based on the ABB-NV correlation form. To account for effects of the smaller guide thimble geometry and variable grid spacing on the non-uniform shape factor, modifications to the WSSV correlation form are made. A description of the Westinghouse CHF tests supporting the WNG-1 correlation is summarized in Section 2 of this report. The database contains test data to support the special geometry terms, especially grid spacing, for the correlation form and for validation.

Section 3 describes the modification of the WSSV correlation form for application with split vanes with a small guide thimble and the optimization of the coefficients for the WNG-1 correlation and the validation of the correlation. As stated above, the correlation form is based on the form used in References 1 and 8 for the ABB-NV, ABB-TV and WSSV correlations. The form is empirical and is based solely on experimental observations of the relationship between the measured CHF and the correlation variables. Similar to the WSSV correlation, the correlation form assumes that there is a linear relationship between CHF and local quality [

]$^{a, c}$. The correlation includes the following variables: pressure, local mass velocity, local quality, a grid spacing term, heated length from inlet to CHF location and the heated hydraulic diameter ratio of the CHF channel. The grid spacing term, GST, is defined as the [

]$^{a, c}$. The heated hydraulic diameter ratio is defined as the [ ]$^{a, c}$. The F_C non-uniform shape factor is also optimized for the split vane data with the small thimble fuel geometry and applied to the correlation to account for the effects of non-uniform axial power shapes [ ]$^{a, c}$.

All test data were evaluated by using the Westinghouse thermal hydraulic code, VIPRE-01 (or VIPRE), Reference 2. VIPRE was used to compute the local coolant conditions for the CHF test sections. A VIPRE model was prepared for each test section and appropriate empirical grid mixing factors for the split vane designs were input into the model.

Section 4 summarizes the statistical evaluation for the WNG-1 correlation and determination of the 95/95 DNBR limit. All the statistical tests are standard statistical methods that have been previously applied for other NRC-approved correlations. Tests for normality were performed to check the hypothesis that the data are normally distributed. Statistical tests were performed to determine if all or selected data groups belong to the same population, in order to be combined for the evaluation of the 95/95 DNBR tolerance limit. Descriptions of the statistical tests applied are given in Section 4. The 95/95 DNBR limit is determined [ ]$^{a, c}$. Since all data grouped by geometry could be pooled, based on the applied statistical tests, the 95/95 DNBR limit for the WNG-1 correlation was based on the final database and determined to be 1.14. Scatter plots of the ratio of measured to predicted (M/P) CHF versus correlation variables were also made to illustrate that the ratio does not show any trends relative to correlation variables.

Section 5 discusses how the WNG-1 correlation is to be applied in plant safety analyses or reload analyses. Conclusions are presented in Section 6 and References are given in Section 7.

A detailed summary of the correlation and validation databases for the WNG-1 correlation is given in Appendix A. The statistical output of the WNG-1 correlation is given in Appendix B. A detailed summary of the test section radial and axial power distributions is given in Appendix C.

Figure 1-1
Description of Split Vane Designs

a, c

2.0 Description of CHF Test Program and Test Section Geometry

All the CHF experiments were conducted at Columbia University's Heat Transfer Research Facility. The WNG-1 correlation is based upon a re-evaluation of CHF data from tests that spanned the period from 1990 to 1996 and new data from tests performed in the period 1998 to 2003. The validation tests for the WNG-1 correlation were performed over the period of 1970 to 2001. A description of the test facility for the later tests, after 1990, can be found in Reference 8. A detailed description of the facility for the tests performed in the 1970's is given in Reference 9.

2.1 Description of Typical Test Sections

The correlation form was based on the WSSV form in Reference 1, but was modified to account for the effects of the split vanes and small thimble, as summarized in Section 3. The data used for the determination of the primary coefficients during development of the WNG-1 correlation were obtained from nineteen test bundles, seven with a uniform axial power shape and twelve with non-uniform axial power shapes. Nine of these test bundles were also used in existing correlations such as the WRB-2M, Reference 3, and the ABB-X2 for European application, Reference 4. The test sections in the correlation database simulate a 5x5 or 6x6 array of the Westinghouse fuel assembly geometry with split vane mixing grids. Sixteen of these test sections are representative of the Westinghouse fuel assembly with 0.374 inch O.D. heated rods, 0.496 inch rod pitch, and 0.474 – 0.482 inch O.D. guide thimble. Two test sections are representative of the Westinghouse fuel assembly geometry with 0.360 inch O.D. heated rods, 0.485 inch rod pitch and 0.471 inch O.D. guide thimble. One test section is representative of the Westinghouse fuel assembly geometry with a 0.423 inch O.D. heated rod and 0.563 inch rod pitch. One test was performed to examine the impact of short grid spacing, two IFM grids in each structural grid span, with the Westinghouse assembly geometry of 0.374 inch O.D. heated rods, 0.496 inch rod pitch and 0.482 inch O.D. guide thimble.

The data used to validate the WNG-1 correlation were obtained from seven test bundles, three with a uniform axial power shape and four with non-uniform axial power shapes. The validation database test sections simulate a 4x4, 5x5 or 6x6 array of the Westinghouse fuel assembly geometry with a split vane design, [ ]$^{a, c}$, mixing grids. The validation database is approximately 29% of the correlation database. The validation database was selected to demonstrate the WNG-1 correlation is robust and predicts data well for conditions that are slightly outside the parameter range in the correlation database. Three of these test bundles were used in the development of the WRB-1 and WRB-2 correlations, References 6 and 7, and have an older Inconel grid design. Additional validation tests (Tests 83 and 102) are split vane designs that are used outside the United States. Five of these test sections are representative of the Westinghouse fuel assembly with 0.374 inch O.D. heated rods, 0.496 inch rod pitch, and 0.474 – 0.482 inch O.D. guide thimble. Two of the test sections are representative of the Westinghouse fuel assembly geometry with 0.422 inch O.D. heated rods and 0.555-0.563 inch rod pitch.

From the total of twenty-six tests examined, twelve of the tests were conducted with a simulated guide thimble and fourteen tests were conducted with simulated matrix subchannels. Typical radial geometries for the 5x5 test sections, with and without a guide thimble, are shown in Figures 2-1 and 2-2. Typical radial geometries for the 6x6 test sections with the small thimble, with and without a guide thimble, are shown in Figures 2-3 and 2-4. A typical radial geometry for the 4x4 test sections, without a guide thimble, is shown in Figure 2-5. The power split between the cold rods and hot rods ranged from [ ] ^{a,c}. The radial power distributions for the individual tests are given in Appendix C. The non-uniform tests were conducted with multiple axial power shapes, as shown in Figure 2-6. The test section heated length for the tests ranged from 96 inches to 168 inches. The upstream grid spacing in the tests ranged from 6.4 inches to 26 inches. The axial locations of the test grids and rod thermocouples for the individual tests are given in Appendix A. A summary of the test section geometry for the twenty-six tests is shown in Table 2-1. The data from the "correlation" test sections were used to develop the coefficients for the WNG-1 correlation. The data from the "validation" test sections were used to validate the correlation. Since Tests 100-102 provided additional data with the larger rod diameter and larger rod pitch, producing increased values of the matrix heated hydraulic diameter, Dhm, these tests were added to the correlation database for the correlation statistical evaluation.

The test grids for all the Westinghouse tests are similar to the production grids of actual fuel designs. Some tests were performed with Zircaloy-4 or ZIRLO™ material and intermediate simple support (SS) grids were used to prevent excessive rod deflection due to electromagnetic forces. Some test grids were made of the stronger Inconel 625 material and the intermediate SS grids were not necessary for minimizing rod bow and deflection.

2.2 Test Procedure and Operation

Although the general test procedure has not changed from earlier tests, a brief description of the test procedures and operation for the more recent tests, after 2001, is provided below:

At the beginning of each test, cold flow pressure drop points were obtained over a range of flow conditions. At the start of each day of testing, a repeat pressure drop point is taken for comparison with earlier data. These data provide isothermal grid span pressure drop values to compare with prediction and establish a base for comparison in case of a malfunction of the rod bundle during the tests.

Heat balances were performed on the test section to check all loop and bundle instrumentation at high temperature and power and to check heat losses. These runs were accomplished at subcooled conditions before mixing or CHF data were obtained at the beginning of each day of operation. Mixing or CHF testing generally was not started until a test section heat loss was [ ] ^{a,c}. Heat loss is defined as the fraction of heat generated by the rods that is lost to the test section shroud walls.

Subchannel mixing data were obtained at non-boiling conditions for each test with a uniform axial power shape. Subchannel thermocouple data were recorded for each mixing test run after steady-state conditions were achieved for a constant pressure, inlet temperature, mass velocity and power. Power was determined for each test condition so the calculated outlet temperature in the hottest subchannel is close to the value specified in the mixing test matrix.

Critical Heat Flux experiments were performed by maintaining the following system conditions constant: test section outlet pressure, inlet temperature, and mass flow rate. The total power to the test section is then increased until a temperature excursion is observed by one or more thermocouples positioned inside the heater rods. The amount of the excursion is approximately 10 to 30°F and varies depending on system conditions. When the excursion is judged to be sufficient for a CHF data point, the power to the test section is reduced. When the temperature excursion is minimal, confirmation of the validity of a CHF point is obtained by observing the temperature decay with power reduction. There is a characteristic temperature decay with time as the CHF zone is rewetted. This evidence is considered confirming in cases where the temperature decay pattern is typical. Otherwise, the experiment is repeated. When a CHF point is observed, the following measurements are recorded, while holding the test section power constant:

1. Recorded manually:
   - test section outlet pressure
   - pressure drop across the Venturi flow meter from a manometer
   - test section pressure drop from a manometer
   - rod(s) experiencing CHF.

2. Recorded by the data acquisition system:
   - test section voltage
   - bus to bus voltage
   - generator amperages
   - inlet temperature
   - outlet temperature
   - outlet pressure transducers
   - turbine flow meter
   - Venturi flow meter transducer
   - test section pressure drop transducers
   - subchannel temperatures
   - heater rod temperatures.

The test matrices were designed to cover a wide range of operating conditions and minimize peripheral rod indications.

Table 2-1
Geometric Characteristics of the WNG-1 Correlation and Validation Tests

Test No.	Test Array	Rod Diameter (~ in)	Rod Pitch (~ in)	Split Vane Type	Heated Length (~ in)	Grid Spacing (~ in)	Guide Thimble	GT Diameter (~ in)	Axial Shape	Radial Split Cold/Hot	Shroud Clearance (~ in)	SS Grid
						Correlation Data						
						Validation Data						

a, b, c

a, b, c

* EPRI Test #, Reference 10, used for Test Identification, Data from References 6 and 7 Applied

Grid Spacing Definitions:

x / y - Two grid spacings, x and y in test

x – y - Multiple grid spacing from x to y. For tests 108 and 109, grid spacings were [ ] a, b, c

xE/y - Generally grid spacing of y, but last grid is x inches from end of heated length (EOHL) for uniform test

Figure 2-1
Typical Radial Geometry
5x5 Matrix Test

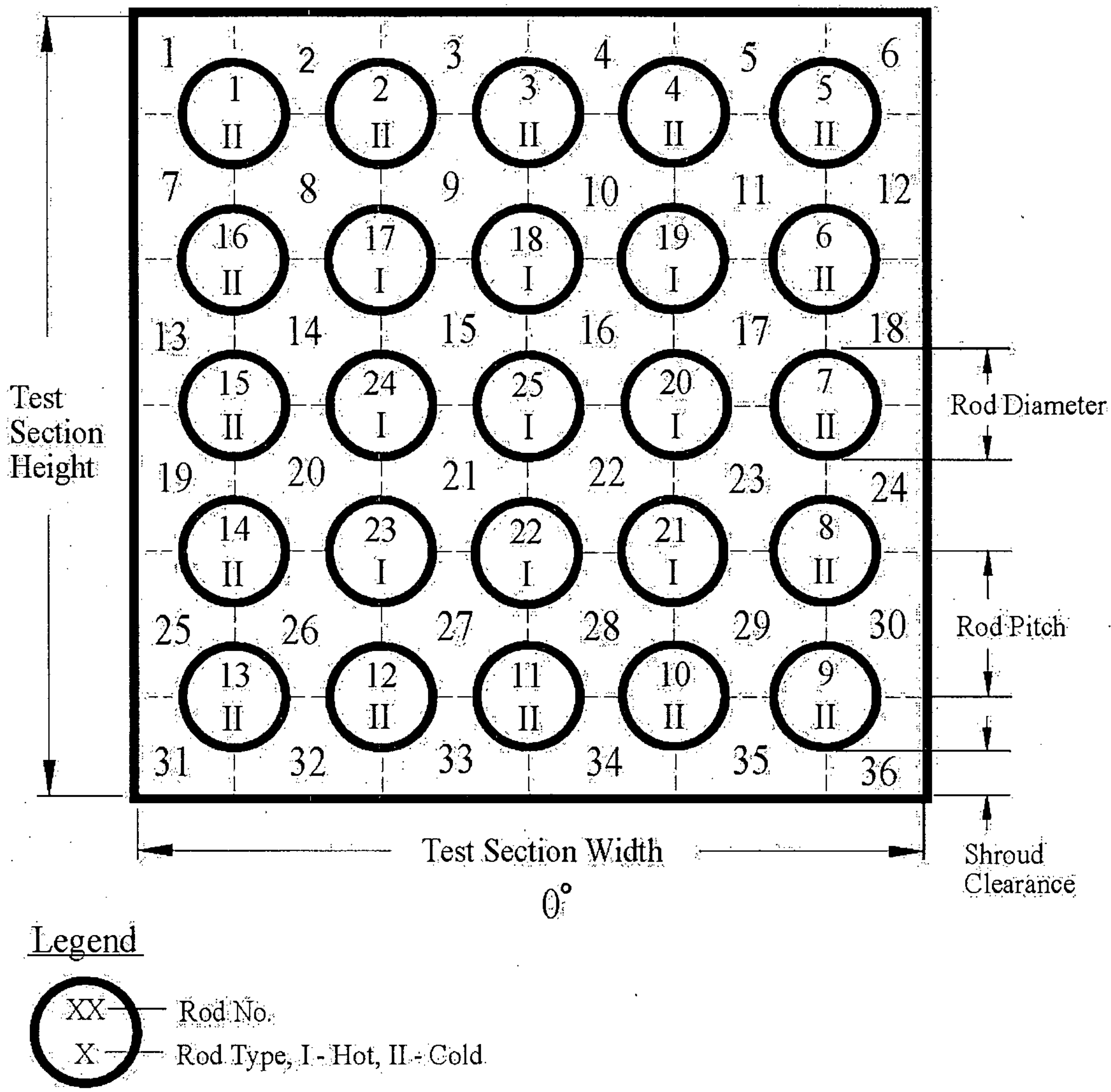

Figure 2-2
Typical Radial Geometry
5x5 Guide Thimble Test

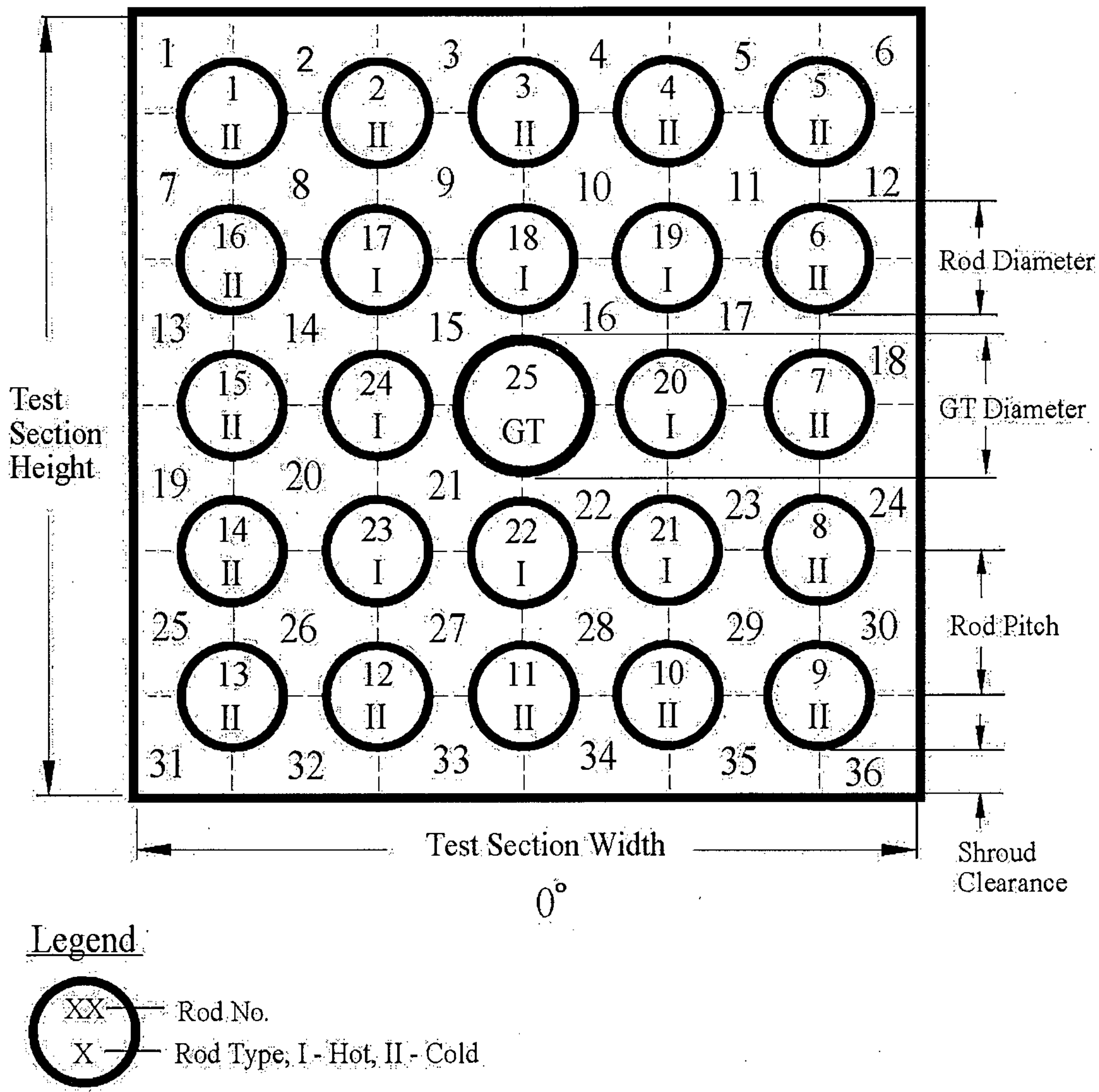

Figure 2-3
Typical Radial Geometry
6x6 Matrix Test

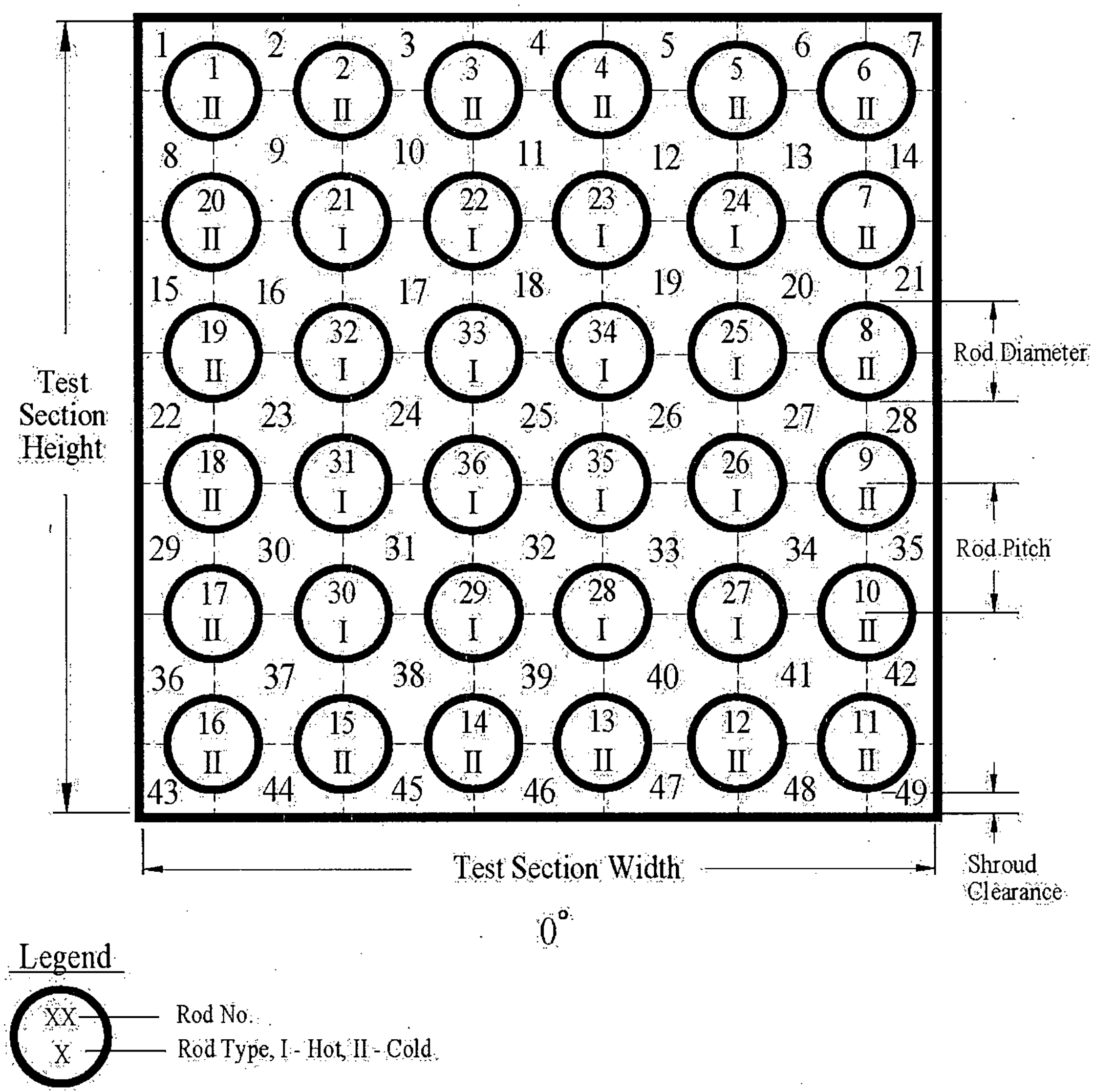

Figure 2-4
Typical Radial Geometry
6x6 Guide Thimble Test

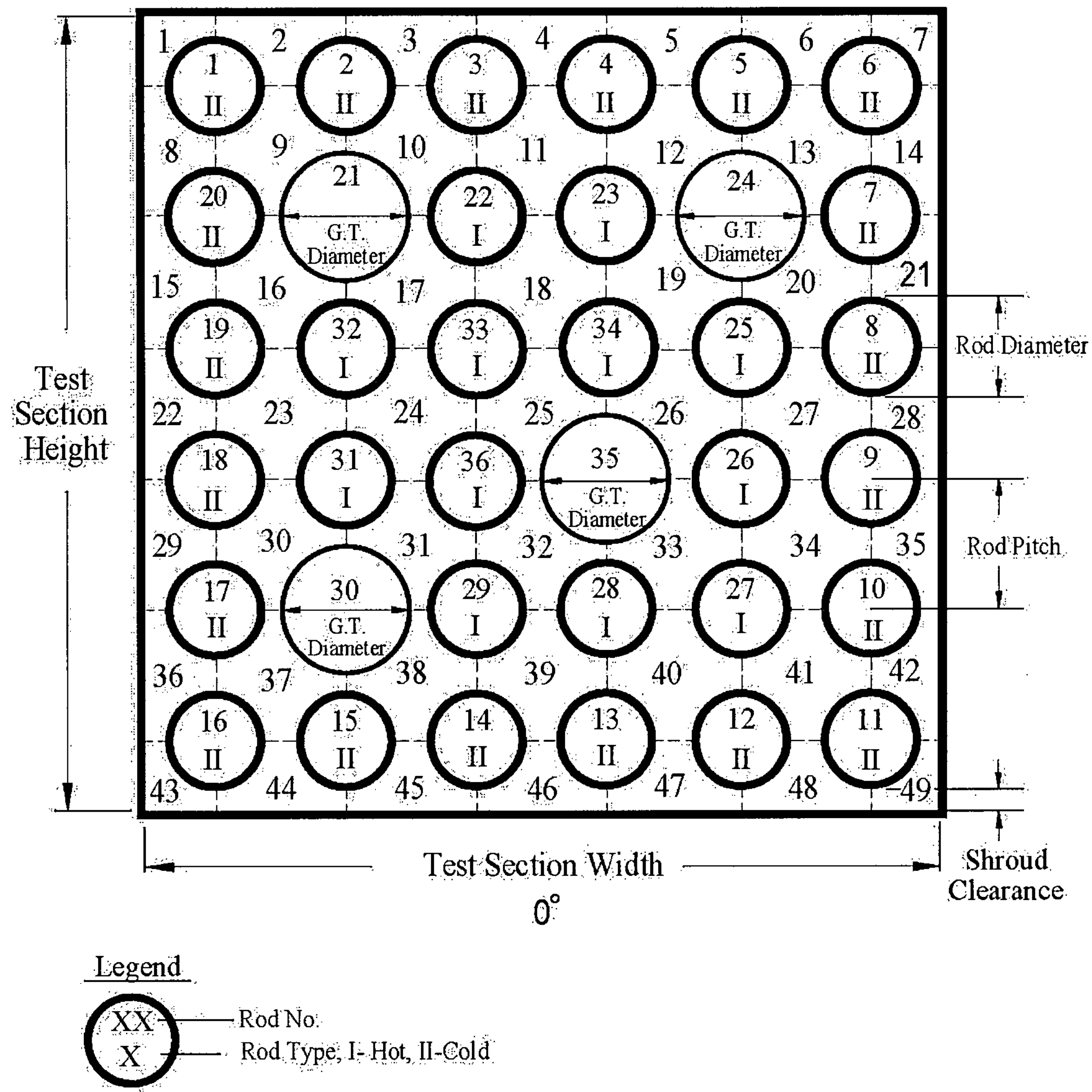

Figure 2-5
Typical Radial Geometry
4x4 Matrix Test

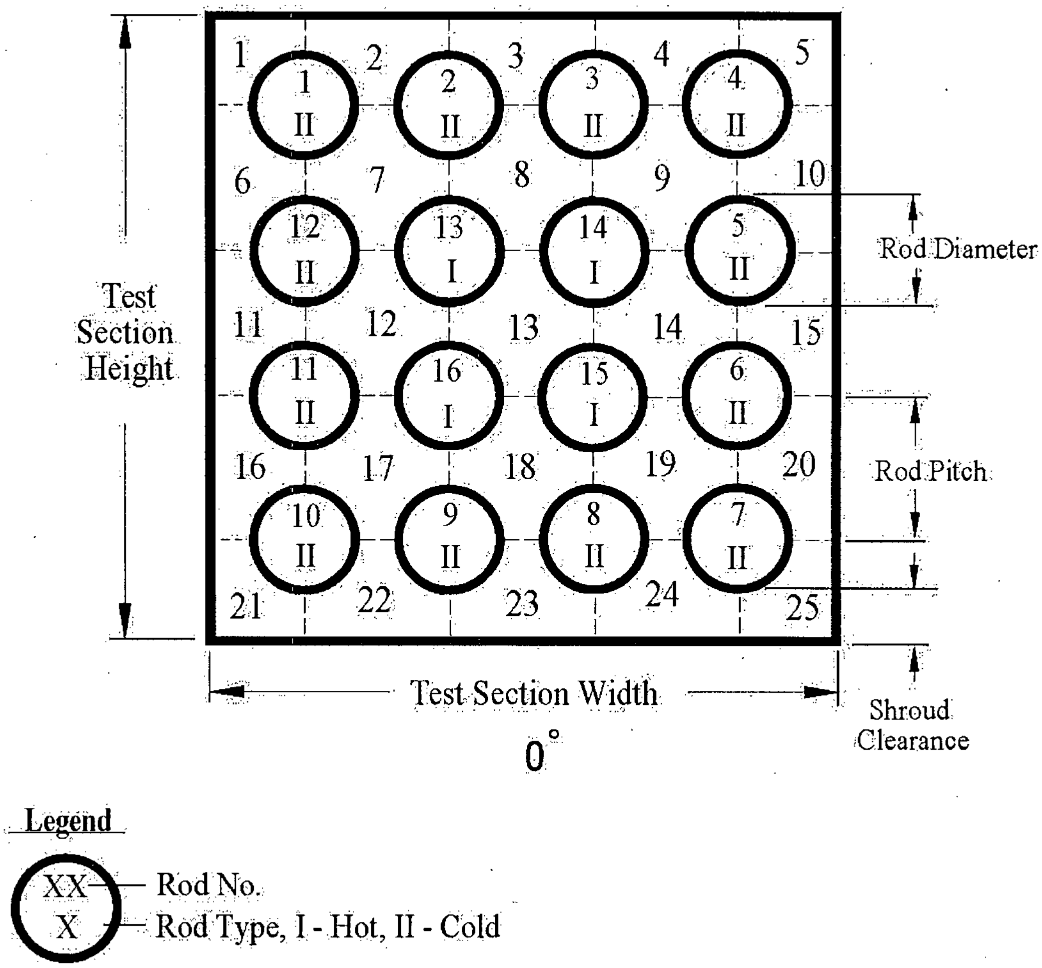

Page Intentionally Left Blank

Figure 2-6
Axial Heat Flux Distribution
Non-Uniform Axial Power Shapes in WNG-1 Database

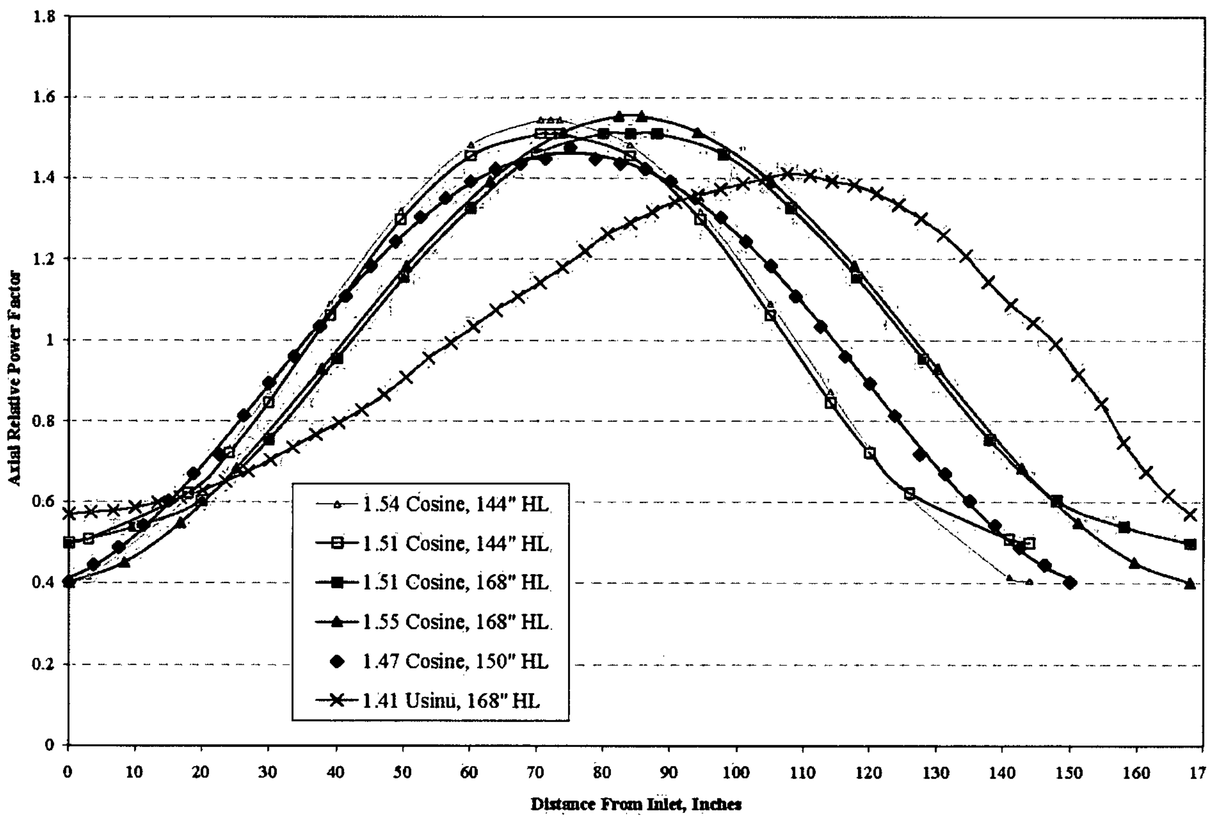

Page Intentionally Left Blank

3.0 Development of WNG-1 Correlation for Split Vane Mixing Grids

The WNG-1 correlation form was developed based on Westinghouse Critical Heat Flux (CHF) test data obtained from the Heat Transfer Research Facility of Columbia University. The tests were performed with simulated 5x5 and 6x6 arrays of Westinghouse fuel designs containing 0 to 2 Intermediate Flow Mixing grids (IFM grids) between the structural mixing grids. All the grids used for the CHF tests contain a split vane mixing grid design, [ ] ^{a,c}, in Figure 1-1. The correlation database includes tests with uniform and non-uniform axial power distributions, with and without guide thimbles, heated lengths from 118.1 to 168 inches and grid spacing from 6.4 to 21.1 inches. A validation database, approximately 29% of the correlation database, was then used to validate robustness of the correlation. The validation database includes tests with uniform and non-uniform axial power distributions, with and without guide thimbles, heated lengths from 96 to 168 inches and grid spacing from 10 to 26 inches.

The functional form of the correlation is based upon the WSSV correlation form developed in Reference 1. To account for some geometric differences in vane design and guide thimble size, the development of the form and application for the WNG-1 correlation are provided in section 3.1. The functional form of the CHF correlation is empirical and is based solely on experimental observations of the relationship between the measured CHF and the correlation variables. Similar to the WSSV correlation, the correlation form assumes that there is a linear relationship between CHF and local quality [

] ^{a,c}.

The correlation includes the following variables: pressure, local mass velocity, local quality, a grid spacing term, GST, heated length from inlet to CHF location and the heated hydraulic diameter ratio of the CHF channel. The grid spacing term, GST, is defined as the [

] ^{a,c}. The heated hydraulic diameter ratio is defined as the [

] ^{a,c}. The F_C non-uniform shape factor is also optimized for the split vane data with the small thimble and applied to the correlation to account for the effects of non-uniform axial power shapes [ ] ^{a,c}.

3.1 Description of Tests Supporting Correlation

A summary of the Westinghouse CHF tests supporting the WNG-1 correlation is provided in Section 2 of this report. Figures showing the geometry of typical 4x4, 5x5 and 6x6 test sections are also shown in Section 2. The array of rods was placed in a square metal shroud lined with unheated ceramic walls. Similar to previous correlations, the WNG-1 correlation is based upon a series of tests that provide a good representation of the thermal performance of Westinghouse fuel assemblies. The tests were run with grids made of Zircaloy material with simple support grids placed between the test grids or with test grids made with the stronger Inconel 600, or 625, material to minimize the rod deformation. Both of these changes provided a good representation of the thermal performance of Westinghouse fuel assembly in the reactor. For the tests in the correlation database, the rod to wall gap was sized to minimize the risk of DNB occurring on peripheral rods that are not representative of the fuel assembly, while maintaining similar hydraulic resistance in the grid region for peripheral and interior subchannels. The relative radial power split between cold and hot rods ranged from approximately [ ]^{a,c} to minimize the risk of DNB occurring on peripheral rods. The radial power split was created by using tubes with different wall thickness. The tubing was heated by passing DC current through the tube walls. Inconel 600 and 625 tubing was used in the construction of the heaters. The heaters were filled with alumina ceramic cylinders to maintain rod geometry, prevent deformation during testing, and to isolate the CHF detecting instrumentation from the tubing inner wall.

For uniform axial power shape tests, cold rods [ ]^{a,c} had a single thermocouple positioned 0.5 inches upstream of the end of heated length. Hot rods (relative power factor 1.00) had quadrant thermocouple instrumentation located 0.5 inches upstream of the end of heated length and a single thermocouple located near mid-span of the last structural grid span. For the non-uniform axial power shape test, non-directional type thermocouples were used in cold and hot rods at various axial levels. The location of the rods with quadrant thermocouple instrumentation and the axial locations of thermocouples for the specific tests are shown in Appendix C.

Mixing tests were also performed for test sections with a uniform axial power shape to determine the empirical mixing factors (inverse Peclet number, Pe, or equivalent Thermal Diffusion Coefficient, TDC) for the split vane grid. To evaluate the subcooled subchannel mixing, a thermocouple was installed in each subchannel at the end of the heated length to measure subchannel outlet temperature. A thermocouple support grid was used to locate these thermocouples in the center of the subchannels.

Since the WNG-1 correlation needed to cover fuel designs with grid spans having 0 to 2 IFM grids, CHF test data for split vane fuel assembly designs from previous testing were included in the correlation database, Table 2-1, to make the correlation robust. The database contains the data from the WRB-2M correlation, Reference 3, and data for the 17x17 and 16x16 designs in Europe, ABB-X2 correlation, Reference 4. The correlation database for the WNG-1 (Westinghouse NGF) correlation was selected from Westinghouse CHF tests based on several criteria:

1. Correlation database includes all data taken with simulated 5x5 arrays for the 17x17 and 16x16 NGF split vane fuel assembly designs.
2. Correlation database should include CHF data from tests that are used to evaluate the split vane mixing data.
3. Correlation database should include CHF data with different rod and hydraulic diameters and guide thimble sizes to expand geometric range.
4. Correlation database should include cosine data for 0.374" rod with one IFM between structural grids to appropriately cover range of 0 to 2 IFM grids per nominal grid span for the 17x17 designs.
5. Correlation should include different heated lengths for uniform axial data to expand quality range.

The correlation database for the NGF split vane correlation, WNG-1, is given in Table 2-1.

The primary intent of the validation was to demonstrate the correlation is robust. To develop a separate validation database for the WNG-1 correlation, validation tests are selected to:

1. Provide additional data for geometry with 0.422 in diameter rod.
2. Provide confirmation that data for the RFA-2 fuel fits the correlation.
3. Provide confirmation that the modification to the non-uniform shape factor is applicable to data from non-uniform tests with a μsinμ axial power shape.
4. Provide confirmation that data from uniform axial power tests with 96" heated length are applicable with the heated length term applied for the correlation.
5. Provide confirmation that correlation can be extended to grid spacing of 22 in and pressure to near 1400 psia.
6. Provide at least 300 data points, or approximately 20% of the correlation database.

To meet these conditions, the seven tests listed in Table 2-1 were selected for the validation database. It is noted that some of the tests are for older grid designs no longer used and for grid designs used only outside of the United States. As stated above, the validation database was selected to demonstrate the correlation is robust. The applicable designs (Section 1.1) are a subset of the correlation database.

3.2 Correlation Form

As stated earlier, the basic form for the WNG-1 correlations is similar to the WSSV correlation developed in Reference 1. Following the development of the WSSV correlation form, the base form of the WNG-1 correlations is developed with the primary variables: pressure, local mass velocity, and local quality. [ ]^{a,c} of the correlation use these primary variables. This [ ]^{a,c} expression is based on a [ ]^{a,c} expression used to develop the final correlation is given below:

a, c

[ ]

where: $q''_{CHF,U}$ = critical heat flux for uniform axial power, MBtu/hr-ft^2
P = Pressure, psia
GL = local mass velocity at CHF location, Mlbm/ hr-ft^2
XL = local coolant quality at CHF location, decimal fraction

This base form can be used to correlate the data from rod bundle test sections without variable grid spacing. Fuel dependent special terms are then developed for Grid Spacing (GS), Distance from Grid (DG), Heated Length (HL) and Heated Hydraulic Diameter (Dhm). As noted in Reference 1, split vane test data were used to provide the form for the grid spacing terms and to fit higher quality data for the WSSV correlation form development. The required terms are then applied to the base form to account for variable grid spacing. The terms are discussed in brief for the application for the WNG-1 correlation. It is noted that the WSSV correlation had a set of terms to account for different performance in a matrix channel adjacent to the large guide thimble and a matrix channel [ ]^{a,c} in the CE-PWR fuel. For the relatively smaller thimble (replaces one rod) geometry in

Westinghouse fuel designs, the impact of the thimble is sufficiently small that the set of correlation terms in the WSSV correlation (Reference 1) to account for the proximity of the matrix channel to the guide thimble are not required, simplifying the correlation.

3.2.1 Heated Length, HL

During the development of the ABB-NV and ABB-TV correlations, the heated length term was developed with uniform axial power data with heated lengths of 48 inches, 84 inches and 150 inches, Reference 8. The heated length term developed was a multiplier to the main expression with an exponential form:

[ ] a, c

where: HL = Distance from beginning of heated length (BOHL) to axial location of CHF

Similar to the WSSV correlation in Reference 1, the [

] a, c. Therefore, the expression and range determined in Reference 8 are also applicable for the WNG-1 correlation. Similar to the WSSV correlation, the heated length value is constrained to be no less than 48 inches since that are no CHF data available below this elevation.

3.2.2 Grid Spacing Terms

The form for the grid spacing terms for the WSSV correlation was developed using the larger split vane database, Reference 1. Therefore, the same form is applied for the WNG-1 correlation. The purpose of the grid spacing terms is to account for the effect of the grid on CHF. This term results in lower CHF just upstream of a spacer grid, which produces better agreement with test results. As described in Reference 1, to account for [ ] a, c was developed, defined as:

[ ] a, c

where: [ ] a, c

As noted in Reference 1, this is similar to the grid spacing term in the WRB-2 correlation, Reference 6. Based upon the fit of the data, it is concluded that the best [ ] a, c for the grid spacing term is shown below:

[ ] a, c

where: A, B = Constants determined with nonlinear regression analysis code

As described in Reference 1, following the application of the grid spacing [ ]^{a,c} to the supplemental split vane data, the resultant M/P CHF ratio data were then examined for trends to determine if any additional term is needed to account for the grid spacing geometric effects. One noticeable trend was the [

]^{a,c}. The [ ]^{a,c} with GST determined above accounted for the average effect of the grid spacing, but did not account for the [

]^{a,c} of the correlation form. Since this term was originally developed with split vane data in Reference 1, this additional term is also applied for the WNG-1 correlation. New coefficients are required to properly account for the split vane mixing grid performance.

3.2.3 Heated Hydraulic Diameter of CHF Channel

For the Westinghouse CE-PWR fuel assembly design, a large guide thimble replaces four fuel rods. It has been shown that there is a difference in performance for the matrix subchannels near the guide thimble and the guide thimble side and corner subchannels. For the ABB-NV, ABB-TV, WSSV and WSSV-T correlations, References 1 and 8, the heated hydraulic diameter term was developed to account for the difference in performance:

[ ]^{a,c}

where: Dhm = Heated hydraulic diameter of a matrix subchannel with the same rod diameter and pitch, in
Dh = Heated hydraulic diameter of the subchannel, in
B = Constant fit with nonlinear regression analysis code

To evaluate whether the same form can be applied to the split vane small thimble geometry, the available data at the maximum quality channel at the measured elevation were examined. The data with a non-uniform shape factor near 1.0 were sorted based on test geometry. The average values of M/P CHF ratio for different grid spacing and different subchannel geometry are computed using a correlation with the developed form for the measured elevation data. The data are summarized in the table below. From the data, it appears the form does properly account for the difference in performance between the matrix channel and the thimble channel. Based upon these results, it is concluded that the [ ]^{a,c} can be used to account for the thimble effect for fuel designs with the small thimble.

Test	Rod Diameter	Dhm	GST	Measured Elevation M/P
[				]^{a,c}

3.2.4 Extension of Correlation to Higher Quality

As stated in Reference 1, a [

] a, c. The plot in Figure 3-1 is an example of the observed trend with split vane data. Based upon the [

] a, c value provided the lowest standard deviation for the split vane data. As a further check, the statistical tests described in Section 4.0 are applied to confirm [

] a, c.

Following Reference 1, to account for the measured [

] a, c. Based upon the split vane data at higher mass velocities, the form used for the WSSV correlation in Reference 1 was [

] a, c is shown below:

[ ] a, c

The value of [ ] a, c

[ ] a, c

Plots of the WNG-1 correlation M/P CHF ratio versus the quality with the form adjustment are shown in Section 4. These plots demonstrate that the adjustment adequately accounts for the flow regime effects at higher qualities.

3.2.5 Optimization of Tong F_C Shape Factor for Non-Uniform Axial Power Shapes

A number of non-uniform tests are included in the split-vane correlation database, Table 2-1. The axial power shapes are shown in Figure 2-6. The data at the measured elevations were examined with correlations developed with uniform axial power shape data and the correlation form:

[ ] a, c

The matrix test data and the guide thimble test data were examined separately to determine whether the same trend is observed in both data sets. The non-uniform data based on local conditions at the measured elevations were examined with the non-uniform shape factor, F_C, set to 1.0 and with the standard Tong non-uniform shape factor with the Tong empirical constants, Reference 5. For the case when the non-uniform shape factor is applied, the predicted CHF is computed with the expression:

$$q''_{CHF,NU} = q''_{CHF,U} / F_C$$

where: $q''_{CHF,U}$ = local critical heat flux in channel predicted by the correlation
F_C = Non-uniform heat flux factor

The value of F_C is determined with the expression:

$$F_C = \frac{C}{q''_{CHF,NU}\,(1-e^{-Cl_{crit}})}\int_0^{l_{crit}} q''(z)\,e^{-C(l_{crit}-z)}\,dz$$

The Tong empirically determined coefficient, C, is evaluated with the expression:

$$C = 1.8 * (1 - XL_{crit})^{4.31} / (GL/10^6)^{0.478}\ ft^{-1}$$

where: $q''_{CHF,NU}$ = non-uniform heat flux at CHF location l_{crit}, MBtu/hr-ft^2
$q''(z)$ = local heat flux versus axial length, MBtu/hr-ft^2
l_{crit} = distance from inlet to CHF location, ft
z = axial length, ft
XL_{crit} = equilibrium quality at CHF locations
GL = mass velocity, Mlbm/hr-ft^2

The overall results for the guide thimble tests are shown in the table below:

a, c

[ ]

Based upon this data, it appears that the non-uniform shape factor required for the non-uniform data to fit the expression developed from uniform data is [ ] a, c. Plots of the average measured/predicted (M/P) CHF ratio using a measured elevation correlation developed from uniform guide thimble data [

] a, c are shown in Figure 3-2. These plots indicate the required non-uniform shape factor value required [

]$^{a, c}$, as shown in Figure 3-2.

The same process applied to the thimble non-uniform test data was followed with the matrix non-uniform data. The matrix data shows a similar trend as the guide thimble data with F_C set to 1.0. Trend plots of the M/P CHF ratio based on the measured elevation correlations versus values of the non-uniform shape factor computed with the Tong empirical coefficients, F_T, are shown in Figure 3-3. Both plots, guide thimble test data and matrix test data, show a very similar trend of M/P close to 1 for F_T close to 1.0 and M/P about 1.2 for F_T near 1.5. This indicates the value of the non-uniform shape factor computed with the Tong empirical coefficients is too large for the split vane data in the WNG-1 correlation database. Consideration was given to modifying the constants in the equation for C, similar to the optimization performed for the side-supported and non-mixing vane data in Reference 8. However, there was no direct allowance for the [

] $^{a, c}$. Therefore, the values of F_C are computed with the expression:

[ ]^{a,c}

where: F_C = Non-uniform shape factor applied to non-uniform axial shape data
F_T = Non-uniform shape factor computed with Tong empirical coefficients
B = Constant fit with nonlinear regression analysis
[ ]^{a,c}

The thimble and matrix channel data were initially correlated separately, and both sets of data had essentially the same value for the constant B, again indicating the same trend for the two test geometries. Based on the lack of trend, as shown in plots in Section 4, the optimization of the non-uniform shape factor [

]^{a,c}.

3.3 Final Correlation Form

Based upon the evaluation of the uniform and non-uniform data, the following form is applied to the split vane test data.

Final WNG-1 Correlation Form

a, c

[ ]

The Departure from Nucleate Boiling Ratio (DNBR) is defined as:

$$DNBR = q''_{CHF,U} / (q''_{Channel} * F_C)$$

where
$q''_{CHF,U}$ = Critical Heat Flux Based on Uniform Axial Power Shapes, MBtu/hr-ft^2
P = Pressure, psia
GL = Local Mass Velocity at CHF, Mlb/ hr-ft^2
XL = Local Coolant Quality at CHF, decimal fraction
Dh = Heated Diameter of Subchannel, inches
Dhm = Heated Diameter of Matrix Subchannel, inches
DG = Distance from [ ]^{a,c} Grid to CHF Location, inches
GS = Grid Span Upstream of Grid Just Upstream of CHF Location, inches
GST = Grid Spacing Term = [ ]^{a,c}
HL = Heated Length From Beginning of Heated Length to CHF Location, inches
$q''_{Channel}$ = Local Heat Flux, Mbtu/hr-ft^2
F_C = Optimized F-Factor To Correct $Q''_{CHF,U}$ for NU Shapes
F_T = Standard Tong Non-Uniform Shape Factor

The Tong non-uniform shape factor, F_T is computed with the empirically determined coefficient, C,

$$C = 1.8 * (1 - XL_{crit})^{4.31} / (GL/10^6)^{0.478} \ ft^{-1}$$

3.4 VIPRE Model

The test data from Columbia were evaluated by using the Westinghouse version of VIPRE-01 (VIPRE) thermal hydraulic code, Reference 2. The VIPRE code was used to predict local coolant conditions in each subchannel for the CHF test sections at multiple axial nodes. VIPRE models were prepared for each test section in the database based upon the test section axial and radial geometry and the test section axial and radial power distributions. The VIPRE calculations were based on the measured values of pressure, inlet temperature, bundle average mass velocity and bundle average heat flux.

The VIPRE decks are set up with [ ]^{a,c} for the non-uniform tests. The [ ]^{a,c} is selected to define the grid locations [ ]^{a,c}. Following the development of the WRB-1, WRB-2 and WRB-2M correlations, References 3, 6 and 7, calculated [

]^{a,c}.

For the uniform axial power shape CHF test programs, approximately 30 mixing points were taken to evaluate the grid mixing factor. Mixing test procedures are described in detail in Reference 11. The tests were performed with the same test arrays used for the CHF tests. The subchannel mixing data were then reduced to evaluate the thermal mixing factor. Since it is [

]^{a,c}.

[ ]^{a,c}

The VIPRE two-phase flow and cross-flow correlations are kept the same as that for Westinghouse fuel design applications in Reference 2. The input specifications for the VIPRE model are summarized in Table 3-2.

3.5 Data Evaluation and Statistics

The following steps were performed for the optimization of the WNG-1 CHF correlation coefficients with the CHF correlation database:

1.) The data from all the tests in the correlation database are reduced with the VIPRE code to obtain local mass flow and quality conditions for all subchannels and multiple axial nodes for each test run. A utility code was then used to select the local conditions from the [ ]^{a,c} from the VIPRE code. This was a [ ]^{a,c}.

The [ ]^{a,c} coefficients for the final correlation form, provided in Section 3.3, were then determined from the [ ]^{a,c} using a nonlinear regression analysis. As discussed in Section 3.2, the coefficients for the heated length term are to be the same as the ABB-NV, ABB-TV and WSSV correlations, References 1 and 8. To provide optimization of the non-uniform shape factor [

]^{a,c}.

2.) The data from the correlation database are then reduced in a version of VIPRE that has the correlation coefficients determined at the [ ]^{a,c}. The data from all the tests in the correlation database are [ ]^{a,c} with the VIPRE code to obtain local mass flow and quality conditions and DNBR calculations for all subchannels and multiple axial nodes for each test run. The local conditions were then [

] [a, c] for each test run. While [ ] [a, c] of the correlation form were optimized using a non-linear regression analysis.

3.) Step 2 was repeated with the WNG-1 correlation in VIPRE having the coefficients determined in step 2. The local conditions were then [ ] [a, c] determined in step 2. The correlation statistics at the MDNBR elevation were evaluated using the coefficients determined in step 2. The [ ] [a, c] coefficients were then re-fit using a non-linear regression analysis and the correlation statistics were computed using the new coefficients. Since the [ ] [a, c], the coefficients determined in step 2 are considered to be final.

Following the same process described in Reference 1, a non-linear regression analysis code was also used to sort and fit the test data. The optimization of the constants was performed on data within the parameter ranges shown in Tables 3-3 and 3-4. The code was also used to [ ] [a, c]. The repeat runs were identified in the Columbia database. To be considered as duplicate data, the [ ] [a, c]. After the initial runs, the code could have been used to separate out outliers, following the procedure described in Section 4. No points in the correlation database were rejected by this procedure as outliers.

The WNG-1 correlation with the final coefficients for application with the VIPRE code is shown on the following page. The means and standard deviations for the M/P CHF ratio for the correlation database and individual test sections are presented in Table 3-3, along with the range of the primary variables. As stated earlier, the statistics for the correlation database are based upon the [ ] [a, c] with the correlation application. The statistical output for the individual test points in the WNG-1 correlation database are provided in Appendix B. Further discussion of the statistical evaluation of the WNG-1 correlation is given in Section 4.

Final Correlation Form and Coefficients for WNG-1 for VIPRE Code

a, b, c

[ ]

Nomenclature:

$q''_{CHF,U}$ = Critical Heat Flux Based on Uniform Axial Power Shapes, MBtu/hr-ft^2
P = Pressure, psia
GL = Local Mass Velocity at CHF, Mlb/ hr-ft^2
XL = Local Coolant Quality at CHF, decimal fraction
Dh = Heated Diameter of Subchannel, inches
Dhm = Heated Diameter of Matrix Subchannel, inches
DG = Distance from [ ] $^{a, c}$ to CHF Location, inches
GS = Grid Span Upstream of Grid Just Upstream of CHF Location, inches
GST = Grid Spacing Term = [ ] $^{a, c}$
HL = Heated Length From Beginning of Heated Length to CHF Location, inches
F_C = Optimized F-Factor to Correct $q''_{CHF,U}$ for NU Shapes,
F_T = Standard Tong Non-Uniform Shape Factor

3.6 Validation of Correlation

An independent validation database was generated from tests excluded from the correlation database to verify performance of the WNG-1 correlation, as described in Section 3.1. Due to the large size of the correlation database, the primary purpose of the validation database is to demonstrate the correlation is sufficiently robust that the correlation provides good agreement with parameters somewhat outside the original correlation database. The geometric characteristics for these tests are summarized in Table 2-1. The validation database was generated in a manner similar to the process used to generate the correlation database [ ] $^{a, c}$.

A VIPRE model was prepared for each validation test section based on the test section axial and radial geometry and test section axial and radial power distributions. The VIPRE calculations were based on the measured values of pressure, inlet temperature, bundle average mass velocity and bundle average heat flux at CHF, as given in Appendix A. For tests documented in References 6 and 7, the [

] ^{a,c}. The local conditions at the [

] ^{a,c}, are used to determine the M/P CHF ratio. For non-uniform tests, the calculated DNB ratio is modified with the [ ] ^{a,c} for the axial shape factor, F_C.

The means and standard deviations for the M/P CHF ratio for the validation database and individual test sections are presented in Table 3-4, along with the range of the primary variables. It is noted that no points were eliminated as an outlier by the procedure described in Section 4 in the validation database. The statistical output for the individual test points in the WNG-1 validation database is provided in Appendix B. Further discussion of the statistical evaluation of the WNG-1 correlation is given in Section 4.

Table 3-1

[ ] a,c Input to VIPRE

a, b, c

[ ]

Table 3-2
Input Specifications for WNG-1 Test VIPRE Model

1. Supplementary DNBRS output file selected: IDNBRS set to 2 or 3 in CONT.6
2. Single phase friction factor: f = [ ] a,c
3. Two-phase flow Friction multiplier: [ ] a,c
4. Two Phase Flow: [ ] a,c
5. Axial Power Distribution:
   Uniform Test, uniform axial power distribution
   Non-uniform Test, non-uniform axial power distribution specific to test
6. Grid loss coefficients used: See Table 3-1
7. The crossflow resistance factor: [ ] a,b,c
   [ ] a,b,c
8. The turbulent momentum factor: [ ] a,c
9. The traverse momentum parameter [ ] a,c
10. The axial flow convergence for external iteration, FERROR set to [ ] a,b,c
11. Turbulent Mixing: [
    ] a,c (this applies to both single and two-phase conditions)
12. Uniform mass velocity was used as the inlet flow option
13. [ ] a,c for non-uniform tests

Table 3-3
CHF Test Statistics for WNG-1 Correlation Database

a, b, c

Test No.	Rod Diameter (~ in)	Rod Pitch (~ in)	Dhm (~ in)	Heated Length (~ in)	GST	Axial Shape	Guide Thimble	WNG-1 N	WNG-1 M/P Mean, μ	WNG-1 M/P Std. Dev.

Parameter Range of Data:

Pressure, psi:	Min.	1485	Max:	2495
Local Mass Velocity, Mlb/hr-ft^2:	Min.	0.79	Max:	3.60
Local Quality:	Min.	−0.21	Max:	0.43

Table 3-4
CHF Test Statistics for WNG-1 Validation Database

Test No.	Rod Diameter (~ in)	Rod Pitch (~ in)	Dhm (~ in)	Heated Length (~ in)	GST	Axial Shape	Guide Thimble	WNG-1		
								N	M/P Mean, μ	S Std. Dev.

a, b, c

Parameter Range of Data:

Pressure, psi:	Min.	1405	Max.	2495
Local Mass Velocity, Mlb/hr-ft^2:	Min.	0.86	Max.	3.72
Local Quality:	Min.	−0.14	Max.	0.33

Page Intentionally Left Blank

Figure 3-1
Split Vane Uniform Matrix Test Data vs. XL
[ ][a, c]

a,b,c

[ ]

Page Intentionally Left Blank

Figure 3-2
Non-Uniform Guide Thimble Data [ ] a,c
for Correlation Based on Guide Thimble Uniform Data

a,b,c

[ ]

Page Intentionally Left Blank

Figure 3-3
Non-Uniform Data Trend with Non-Uniform Shape Factor Computed with Tong Coefficients, F_T

[ ]a,b,c

Page Intentionally Left Blank

Figure 3-4
TDC [ ] [a,c], Split Vane Designs

a,b,c

Page Intentionally Left Blank

4.0 Statistical Evaluation

The mean and standard deviation for the ratio of measured to WNG-1 predicted CHF are shown in Table 3-3 for the correlation database and the individual test sections and Table 3-4 for the validation database and individual test sections. A statistical evaluation is performed with the WNG-1 correlation for [ ] a, c, the correlation database, the validation database, and a combined database. To demonstrate that the correlation is robust, [ ] a, c the final combined database. The statistical tests applied are the same tests applied in References 1 and 8 for the ABB-NV, ABB-TV, and WSSV correlations. The data in the correlation database, validation database, and final combined database were examined to determine whether any data would be eliminated as an outlier per the procedure given in Chapter 17 of Reference 12, the same rigorous outlier test applied in References 1 and 8. No points from either the WNG-1 correlation database or the validation database were eliminated by this test.

Section 4.1 describes statistical test methods and procedures, similar to those in References 1 and 8, used for evaluation of the WNG-1 correlation. Section 4.2 provides results of the statistical evaluation and the correlation 95/95 DNBR limit.

4.1 Statistical Tests

Statistical tests were performed to determine if all or selected data groups belong to the same population, for the evaluation of the 95/95 DNBR limit. For normally distributed groups, homogeneity of variance was examined using Bartlett's test and homogeneity of the means was examined with the t-Test or general F-Test. The t-Test with equal variances, Reference 14, was applied for testing the equality of means of two groups that passed both the normality tests and the homogeneity of variance test. The t-Test with unequal variances, Reference 15, was applied for testing the equality of means of two groups that passed the normality tests but failed the homogeneity of variance test. The ANOVA F-Test was applied to multiple groups that passed the normality tests. For groups that did not pass the normality test, the Wilcoxon-Mann-Whitney Test or the Kruskal-Wallis One-Way Analysis of Variance by Ranks Test is used to test the null hypotheses that the medians, or averages, of the tests or groups are the same. The Wilcoxon-Mann-Whitney Test was applied for testing the combine-ability of two groups and the Kruskal-Wallis One-Way Analysis of Variance by Ranks Test was applied to multiple groups. For groups that failed the D' Normality Test but passed other normality tests such as the Kolmogorov-Smirnov Test, the Bartlett and F-Tests were applied to check for poolability of these groups. Data that did not pass any of these tests were not combined.

The one-sided 95/95 limits were calculated for a combined correlation and validation database using data for current grid designs, after the data sets in the database were evaluated to be poolable. The poolability tests were performed on the correlation and validation databases. The poolability tests were then applied [ ] a, c for the tests in the combined database. For normally distributed groups, Owen's one-sided tolerance limit factor, Reference 16, is used to compute the 95/95 DNBR limit. For groups that are not normally distributed, a distribution-free or non-parametric limit, from Chapter 2 of Reference 12, is established. To cover all regions with the 95/95 limit, the most conservative limit for any subset examined is applied to the entire set of data.

Scatter plots were then generated as measured to correlation predicted CHF ratio versus each of the variables in the correlation to examine the correlation for trends or regions of non-conservatism. The DNBR limit is also shown on these plots to show the number of test points that fall below the limit and the location of those points. The total number of test points that fall below the limit is also identified.

4.1.1 Treatment of Outliers

Each database is examined for outliers by the following method:

The probability of rejecting an observation when all data belong to the same group, α, was selected to be 0.05. The term $\alpha' = 1 - (1-\alpha)^{1/n}$ is computed. The value of $(1 - \alpha'/2)$ is the normal cumulative distribution value, P, and the value of $z_{1-\alpha'/2}$ is calculated or taken from cumulative normal distribution tables. For a mean value of m, the values of a and b are computed where:

$$a = m - \sigma * z_{1-\alpha'/2}$$
$$b = m + \sigma * z_{1-\alpha'/2}$$

Any observation that does not lie in the interval a to b is rejected. The method does assume a normal distribution and the values of μ, mean of the data, and s, standard deviation of the data, are reasonable estimates of m and σ. Therefore, care must be taken to ensure the elimination of outliers is justifiable. Based upon the application of this test to the correlation database, validation database and final combined database, no points were eliminated by this test.

4.1.2 Normality Tests

The W and D' tests, Reference 13, were used to evaluate the assumption of a normal distribution. For individual tests with less than 50 test points, the W test is applied. The test statistic W is computed as:

$$W = b^2 / S^2$$

where:

$$S^2 = \sum_{i=1}^{n} (x_i - \bar{x})^2$$

$$b = \sum_{i=1}^{k} a_{n-i+1} (x_{n-i+1} - x_i) \qquad x_i \text{ in ascending order}$$

a_i from Table 1, Reference 13

$k = n/2$ if n is even and $k = (n-1)/2$ if n is odd

The value of W is compared with percentage points of the distribution of W for P set to 0.05 from Table 2 of Reference 13. Small values of W indicate non-normality. For combined tests or individual tests with $n \geq 50$, the D' normality test is applied. The test statistic D' is computed as:

$$D' = T/S$$

where:

$$S = \left[\sum_{i=1}^{n} (x_i - \bar{x})^2 \right]^{0.5}$$

$$T = \sum_{i=1}^{n} \{ i - (n+1)/2 \} x_i \qquad x_i \text{ in ascending order}$$

The calculated value of D' is compared with the percentage points of the distribution of D' from Table 5 of Reference 13. The D' test indicates non-normality if the calculated value of D' falls outside of the range established from Table 5 for P set to 0.025 and 0.975. These tests were selected since they are considered to be more rigorous compared to other normality tests such as the Kolmogorov-Smirnov test. Furthermore, the D' and W tests are the ANSI standard tests that have been used in previous data analyses reviewed and approved by the NRC.

4.1.3 Statistical Tests for Comparison of Data Groups

Statistical tests were performed to determine whether data groups could be considered to come from one population. The Bartlett test for homogeneity of variances and the t-Test, for 2 groups, or the F-Test, for multiple groups are applied to determine if data groups can be combined. If the data groups fail the normality test, the Mann-Whitney Rank Sum test or the Kruskal-Wallis One-Way Analysis of Variance by Ranks test is used to check the null hypotheses that the medians, or averages, of the tests or groups are the same. The Kruskal-Wallis One-Way Analysis of Variance by Ranks test is also used to check the null hypotheses that the medians, or averages, of the tests or groups are the same for multiple groups that pass the normality test, but fail the homogeneity of variance test. For the groups that pass the equality of means tests or the non-parametric tests for the null hypothesis that the samples are from the same population, the normality tests are applied to the combined groups to check the assumption of normality. If the combined group passes the normality test, Owen's one-sided tolerance limit factor, Reference 16, is used to compute the 95/95 DNBR limit. If the combined group fails the normality test, a distribution-free one-sided 95/95 limit is determined, Chapter 2 of Reference 12. A brief description of the comparison tests is given below:

4.1.3.1 Homogeneity of Variances

One of the most used tests for examining the homogeneity of a set of variances is Bartlett's test (Reference 17). Bartlett showed that for a set of variances estimated from K independent samples from normal distributions having a common variance σ^2, a quantity M/C would have a distribution satisfactorily approximated by the χ^2 distribution. Specifically:

$$M = N \ln\left\{N^{-1} * \sum_{t=1}^{K} v_t s_t^2\right\} - \sum_{t=1}^{K} v_t \ln s_t^2$$

$$C = 1 + \frac{1}{3(K-1)}\left\{\sum_{t=1}^{K} \frac{1}{v_t} - \frac{1}{N}\right\}$$

where: s_t^2 is an estimate of variance for test section t based on degrees of freedom v_t, K is the number of test sections,

$N = \sum_{t=1}^{K} v_t$;

and the quantity M/C is distributed approximately as χ^2 with K-1 degrees of freedom.

4.1.3.2 Test for Equality of Means for Two Data Groups - Unpaired t-Test

When data from two groups passed the test for homogeneity of variances, the t-Test was employed to test the hypothesis that $\mu_1 - \mu_2 = 0.0$ or that $\mu_1 = \mu_2$, where μ_1 is the mean from data group 1 and μ_2 is the mean from data group 2. The test statistic t is calculated with the expression:

$$t = \frac{\mu_1 - \mu_2}{s_0 (1/n1 + 1/n2)^{0.5}}$$

where: $s_0^2 = \frac{\sum_{j=1}^{n1}(x_{1j} - \mu_1)^2 + \sum_{j=1}^{n2}(x_{2j} - \mu_2)^2}{n1 + n2 - 2}$ is a "pooled" estimate

The computed value of t is compared with the value $t_{\alpha/2, n1+n1-2}$ in a table of percentiles of the t distribution for α set to 0.05. The hypothesis that $\mu_1 = \mu_2$ is rejected if the computed value of t is larger then the value of $t_{\alpha/2, n1+n1-2}$.

When data from two groups passed the test for normality, but not the test for homogeneity of variances, a t-Test with unequal variances described below was employed to test the hypothesis that $\mu_1 - \mu_2 = 0.0$ or that $\mu_1 = \mu_2$ where μ_1 is the mean from data group 1 and μ_2 is the mean from data group 2. From Reference 15, the test statistic t is calculated with the expression:

$$t = \frac{\mu_1 - \mu_2}{(S_1^2/n1 + S_2^2/n2)^{0.5}}$$

where: S_i^2 = Variance of sample i

ni = Number of data, sample i

4.1.3.3 Test for Equality of Means for Multiple Data Groups – Analysis of Variance, F-Test

An analysis of variance test was performed to test the equality of means and determine whether the data from multiple tests or groups could be pooled. One of the usual techniques for examining the equality of means determined in an experimental study is a particular form of the F-test. In this technique, two mean squares are found, call them S_1, the between test section mean square and S_2, the within test section mean square. If K is the number of test sections, n_t the number of data for test section t and n is the total number of data.

$$S_1 = \frac{\sum_{t=1}^{K} n_t(\overline{X}_t - \overline{\overline{X}})^2}{K-1}, \text{ and}$$

$$S_2 = \frac{\sum_{t=1}^{K}\left\{\sum_{i=1}^{nt}(X_{ti} - \overline{X}_t)^2\right\}}{n-K}$$

In these expressions X_{ti} is an individual datum for test section t, $\overline{X}_t$ is the mean value of X for test section t and $\overline{\overline{X}}$ is the grand mean for all data. Under the hypotheses of normality, homogeneity of variance and equality of means, S_1 and S_2 are independent estimates of the variance, σ^2, due to random deviation from the true grand mean. Therefore the ratio:

$F = S_1 / S_2$ should follow the F distribution with degrees of freedom
$v_1 = K - 1$ and $v_2 = n - K$

The calculated value of F is compared with the value of $F_{1-\alpha}(v_1, v_2)$ for α set to 0.05. Should the test section means not be equal, S_1 will contain additional components of variance. Therefore, large values of F require the rejection of the hypothesis of equality among the means of the tests or groups.

4.1.3.4 Distribution Free Comparison of Average Performance

For combinations that have one or both tests fail the normality test, the Wilcoxon-Mann-Whitney Test, References 12 and 18, is used to compare two groups. To apply this test when one of the samples has $n > 10$, all groups considered, the data are combined. The number of points in the smaller sample is m; the number from the larger group is n. The M/P CHF values from the two groups are ranked from 1 to $m + n = N$ with tied ranks being assigned the average. The value of T is computed by summing the ranks in the smaller group. The value of z is then computed with the expression:

$$z = \frac{T \pm 0.5 - m^*(N+1)/2}{[m^*n^*(N+1)/12]^{0.5}}$$

The significance of z is assessed from cumulative normal distribution table. The value of z must fall between -1.645 to +1.645 for the two groups to pass the null hypotheses that the groups are drawn from the same population for P equal 0.950 for the left and right tails of the distribution.

For comparison of tests or multiple groups that failed the Bartlett test for equal variance or the D' test for normality, the Kruskal-Wallis One-Way Analysis of Variance by Ranks test, References 12 and 18 is used. The level of significance of the test, α, is selected to be 0.05. The $\chi^2_{1-\alpha}$ value for K-1 = degrees of freedom is taken from a table of the percentiles of the χ^2 distribution. The data from all tests or groups are ranked from lowest to highest. The H statistic is then calculated with the equation:

$$H = \frac{12}{N(N+1)} * \sum_{i=1}^{K} \frac{R_i^2}{n_i} - 3*(N-1)$$

where R_i is the sum of the ranks for the ith test, n_i is the number of points in test i and N is the total number of points. If $H > \chi^2_{1-\alpha}$, one rejects the hypothesis that the averages are the same.

4.1.4 One-sided 95/95 DNBR Limit

All data from the correlation and validation databases could be considered in the establishment of the one-sided 95/95 DNBR tolerance limit if the data can be pooled. Therefore, the comparison tests are performed on the combined data sets and grouped data based on geometry prior to the determination of the 95/95 DNBR limit. If not all of the data could be pooled, the data were separated into subsets that could be pooled and the 95/95 DNBR limit was established for the different groups of pooled data. The computed 95/95 DNBR limit for the class of data provides 95% probability at the 95% confidence level that a rod in that class having that DNBR will not experience CHF. The most conservative limit determined for any group of data examined is then applied to the entire correlation data set. For normally distributed groups, Owen's one-sided tolerance limit factor, Reference 16, is used to compute the 95/95 DNBR limit. For groups that are not normally distributed, a distribution-free or non-parametric limit, from Chapter 2 of Reference 12, is established.

4.1.4.1 Normally Distributed 95/95 DNBR Limit

The mean and standard deviation of the ratio of measured to WNG-1 predicted CHF are computed for each data group or class of data that pass the comparison tests and D' normality test. This group can include all data from the correlation database and validation database or a subset of that data. A 95/95 DNBR limit is evaluated for each group based on the following formulas:

$$DNBR_{95/95} = \frac{1}{\overline{X} - KS}$$

$$K = \frac{1.645 + 1.645[1-(1-\frac{2.706}{2(n-1)})\bullet(1-\frac{1}{n})]^{0.5}}{1-\frac{2.706}{2(n-1)}}$$

where: $\bar{X}$ = mean of ratio of measured to predicted CHF
S = standard deviation of measured to predicted CHF
K = 95/95 confidence multiplier (expression given in Reference 14, practically equivalent to Owen's tables in Reference 16)
n = number of data points

4.1.4.2 Distribution Free 95/95 Limit

For data groups that do not pass the D' normality test, a distribution free one-sided 95/95 limit is established. Table A-31 of Reference 12 gives the largest value of m such that one can assert with 95% confidence that 95% of the population lies above the m^{th} smallest value of X_i where X_i is an individual test run value of the ratio of measured to correlation predicted CHF in the non-normally distributed group.

As stated earlier, if all of the data in the combined correlation and validation database could not be pooled, the most conservative 95/95 limit for any subset of that data is the specified limit for the correlation. As a check on the limit, the total number and percentage of test points that fall below the specified limit are also identified. In addition, the limit computed for the entire database is computed using the total variance approach applied in References 6 and 7. Also, the limit for the entire database is computed using the distribution free method if the entire database is not normally distributed.

4.1.5 Graphical Verification

After the determination of the 95/95 DNBR limit for the correlation, scatter plots are then generated for each of the variables in the correlation to examine the correlation for trends or regions of non-conservatism. The M/P CHF ratio is plotted as a function of pressure, local mass velocity, local quality, matrix heated hydraulic diameter, Dhm, heated hydraulic diameter, Dh, the grid spacing term, GST, heated length from BOHL to location of CHF, and the optimized non-uniform shape factor, F_C. The DNBR limit is also shown on these plots to show the number of test points that fall below the limit and the location of those points.

4.2 WNG-1 Correlation Statistical Evaluation and 95/95 DNBR Limit

Following References 1 and 8, the W and D' Normality tests and comparison tests described in Section 4.1 were performed to determine if the WNG-1 correlation and validation data were random samples from one or more populations and whether the data from individual tests and the combination of tests were normally distributed. The initial evaluation was performed to determine whether the correlation and validation data were from the same population to determine whether the validation database did validate the correlation. If the data are from the same population, this allows some or all of the validation database to be combined with the correlation database prior to further examinations for bias and the one-sided 95/95 DNBR limit. The mean and standard deviation for the ratio of measured to WNG-1 predicted CHF are shown in Table 3-3 for the correlation database and Table 3-4 for the validation database. The correlation database has 1,412 points and the validation database has 412 points or 29% of the correlation database. Test for normality of the data for the correlation and validation databases were performed and the results are given in Table 4.2-1. Although the correlation database did not pass the normality test, the Bartlett Test and t-Test were applied to the correlation and validation data along with the distribution free Wilcoxon-Mann-Whitney Test for group comparisons since the correlation data passed other normality tests such as the Kolmogorov-Smirnov Test. The results from the comparison tests are summarized in Table 4.2-2. When correlation and validation tests passed the normality test but failed the Bartlett test, the t-Test with unequal variances was used to test for equality of means. The Wilcoxon-Mann-Whitney Test was also used to test the hypothesis that the two groups could have the same average performance. Based upon this evaluation, it is concluded that the validation database does validate the correlation.

As stated previously, to check the robustness of the correlation, some of the data in the validation database are from tests with [

]$^{a, c}$. The WNG-1 correlation 95/95 DNBR limit is determined [ ]$^{a, c}$. Therefore, the validation data [

]$^{a, c}$ are added to the correlation database to produce the combined database used to determine the 95/95 DNBR limit. [

]$^{a, c}$ to the correlation database to determine the 95/95 DNBR limit.

The results of the parametric comparison tests for the combined database used to determine the 95/95 DNBR limit for the correlation are given in Table 4.2-3. The results indicate that [

]$^{a, c}$. Additional statistical tests were then performed with the test data grouped by test geometry. The database has data from guide thimble tests and matrix tests; so test section geometry is one variable examined. The database has data for tests sections with [

]$^{a, c}$ is another variable examined. The database has data for [

]$^{a, c}$ that is examined. Multiple comparison tests are performed to identify data groups that can be pooled with the application of the statistical tests identified in Section 4.1.

The first step was to examine each geometric group in the database with the normality tests. The results from these normality tests are given in Table 4.2-4. The next step was to examine equality of variance for the groups. The data for the [ ] a, c. There were three sets examined, the [ ] a, c. The results of the Bartlett test are given in Table 4.2-5. Based upon this test, the data grouped by [ ] a, c the Bartlett test for equality of variances, [ ] a, c. Since the data grouped [ ] a, c was applied to test the equality of means. Since the data grouped by [ ] a, c was applied for the comparison of means test. This test was also applied to the data grouped by [ ] a, c. The data grouped by [ ] a, c. The results of the comparison tests are given in Table 4.2-7. Based upon these tests, the data grouped by [ ] a, c could all be pooled. Therefore, for each [ ] a, c, the 95/95 DNBR limit is based on the entire database of 1581 points in Table 4.2-3.

Since the combined database [ ] a, c is based on the parametric method described in Section 4.1. The one-sided 95/95 DNBR limit for the WNG-1 correlation is computed to be 1.139, as shown in Table 4.2-8. Therefore, the 95/95 DNBR limit is set to 1.14. A plot of the measured CHF versus the WNG-1 predicted CHF for all the test data is given in Figure 4.2-1, along with the DNBR limit curve. The DNBR limit of 1.14 is equivalent to a value of 0.8772 for the M/P CHF ratio. It is noted that for the entire database, fifty-six test points, or 3.5% of the data fall below the $M/P_{95/95}$ limit of 0.8772.

The data are then examined graphically in order to check for any deviation as a function of the correlation variables. The plots of the M/P CHF ratio as a function of pressure, local mass velocity, local quality, matrix heated hydraulic diameter, Dhm, heated hydraulic diameter, Dh, the grid spacing term, GST, the heated length from BOHL to location of CHF, and the optimized non-uniform shape factor, F_C, are shown in Figures 4.2-2 through 4.2-9. The DNBR limit is also shown on these plots to show the number of test points that fall below the limit and the location of those points. There are no observed adverse trends on any of the plots.

Based upon the results of the statistical tests applied to the WNG-1 VIPRE database and the scatter plot analysis, the one-sided 95/95 DNBR limit is determined to be 1.14. The applicable parameter ranges for the WNG-1 correlation are given in Table 4.2-9.

Table 4.2-1
W and D' Normality Tests
WNG-1 Database

Data	N	Mean	D' Calculated	D' P=.025	D' P=.975	Pass Test

a, b, c

Data	N	Mean	*W* Calculated	*W* P=.05	Pass Test

a, b, c

Table 4.2-2
Comparison Tests
WNG-1 Correlation and Validation Database

Bartlett Test Results – WNG-1 Data

Database	N	Mean	s	K	M	C	M/C	$\chi^2_{.95}$	Pass Test

a, b, c

Table 4.2-3
Parametric Comparison Tests
Combined Correlation and Validation WNG-1 Database

Test No.	Rod Diameter (~ in)	Rod Pitch (~ in)	Dhm (~ in)	Heated Length (~ in)	GST	Axial Shape	Guide Thimble	WNG-1 N	WNG-1 M/P Mean, μ	WNG-1 M/P Std. Dev.

a, b, c

Bartlett Test Results – WNG-1

Database	N	Mean	s	K	M	C	M/C	$\chi^2_{.95}$	Pass Test
ALL	1,581	1.0027	0.0730	22	122.86	1.0069	122.01	32.6	No

F-Test Results – WNG-1 Data

Database	n_1	n_2	S_1	S_2	S_1 / S_2	$F_{95}(n_1, n_2)$	Pass Test
ALL	21	1559	0.0290	0.00501	5.792	1.57	No

Table 4.2-4
WNG-1 Final Database [ ] a, c Normality Test Results

Data	N	Mean	D' Calculated	D' P=.025	D' P=.975	Pass Test

a, b, c

Table 4.2-5
Bartlett Equality of Variance Test Results, WNG-1

Tests	df	M	C	M/C	$\chi^2_{.95}$	Pass Test

a, b, c

Table 4.2-6
Parametric Comparison Tests for Pooled [ ] a, c Subsets
WNG-1 Database

t-Test Results with Unequal Variance Data Grouped by Test Geometry

a, b, c

Geometry	n_1	n_2	S_1^2	S_2^2	t	$t_{.025,1579}$	Pass Test

Table 4.2-7
Distribution Free Comparison Tests for Pooled [ ] a, c Subsets
WNG-1 Database

Check of H Statistic From Kruskal-Wallis Variance By Ranks Test

a, b, c

Test	n_t	R_i	R_i^2/n_i	H	$\chi^2_{.95}$

Table 4.2-8
Determination of 95/95 DNBR Limit for Pooled Data
WNG-1 Database

Database	N	Mean	S	K	$DNBR_{95}$
[					]

a, b, c

Table 4.2-9
Parameter Ranges for the WNG-1 Database

Parameter	Applicable Range
Pressure (psia)	1405 to 2495
Local Coolant Quality	≤ 0.43
Local Mass velocity (Mlb/hr-ft^2)	0.79 to 3.72
Matrix Heated Hydraulic Diameter, Dhm (inches)	0.46 to 0.53
Heated Hydraulic Diameter Ratio, [ ]$^{a, c}$	0.85 to 1.00
Heated Length, HL (inches)	48* to 168
Grid spacing (inches)	6.4 to 26
Grid Spacing Term, GST [ ]$^{a, c}$	≥ 26.5**

* Set as minimum HL value, applied at all elevations below 48 inches

** If Grid is in next node and GST < 26.5, set GST to 26.5
Note: This does not apply to [ ]$^{a, c}$

Page Intentionally Left Blank

Figure 4.2-1
Measured and Predicted Critical Heat Fluxes
WNG-1 Correlation

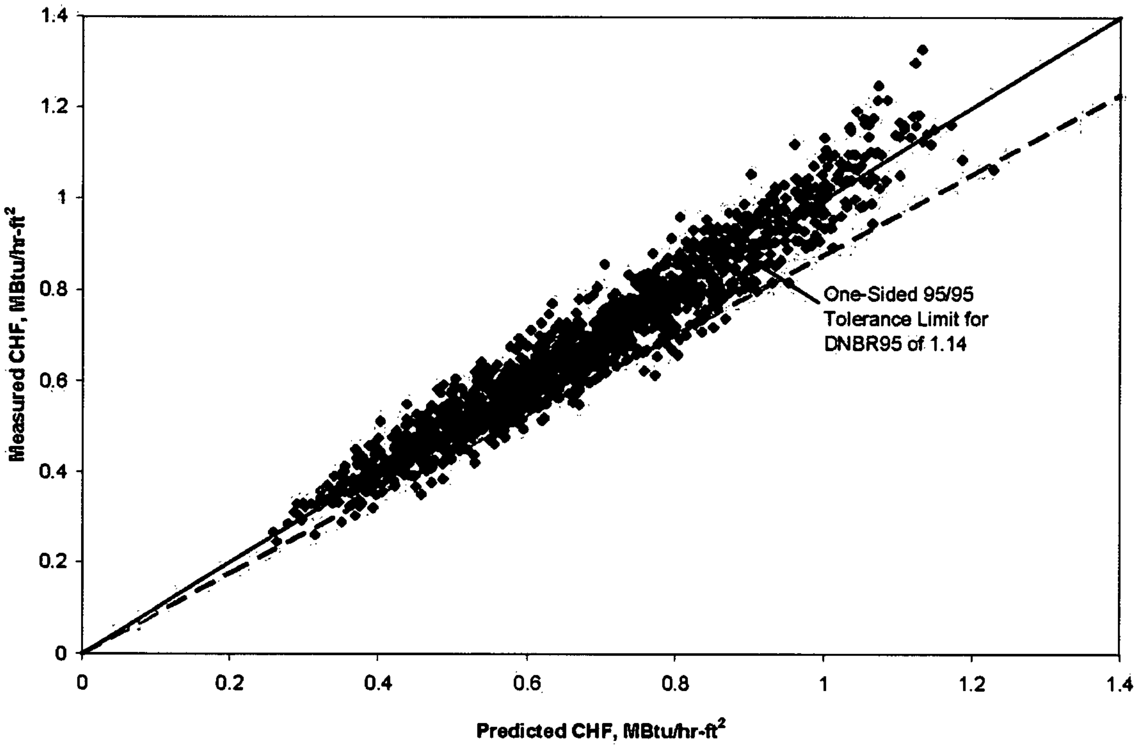

Page Intentionally Left Blank

Figure 4.2-2
Plot of M/P CHF Ratio vs. Pressure
WNG-1 Correlation

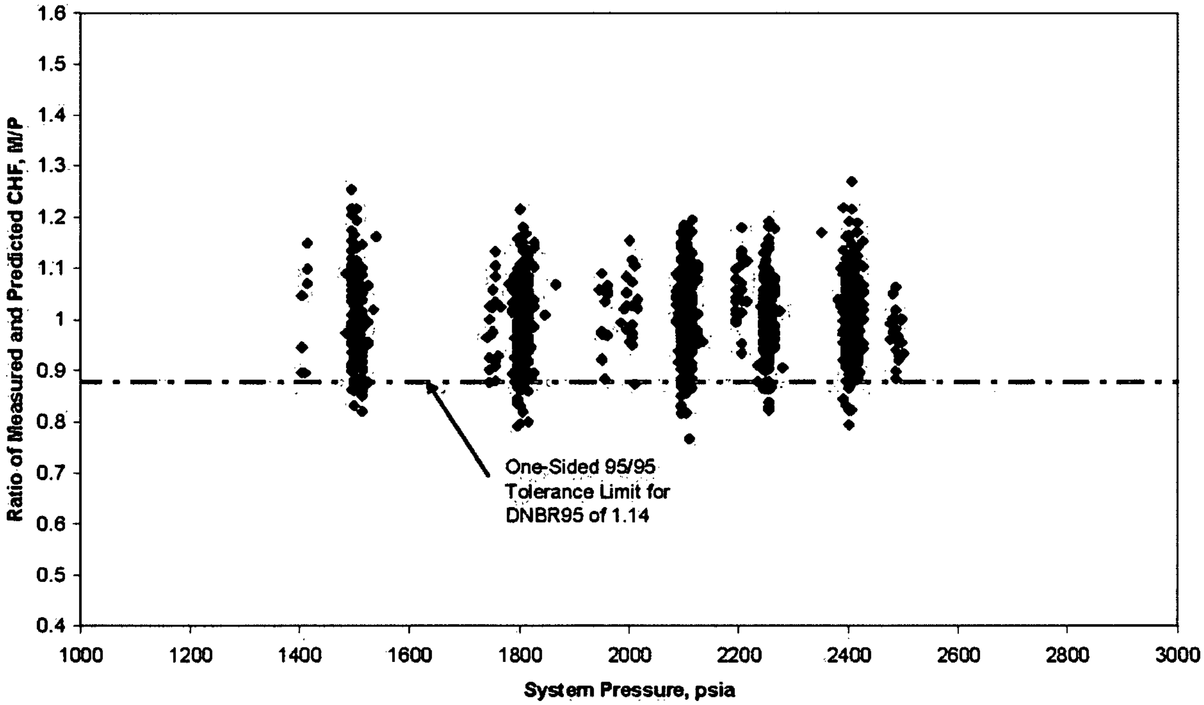

Page Intentionally Left Blank

Figure 4.2-3
Plot of M/P CHF Ratio vs. Local Mass Velocity
WNG-1 Correlation

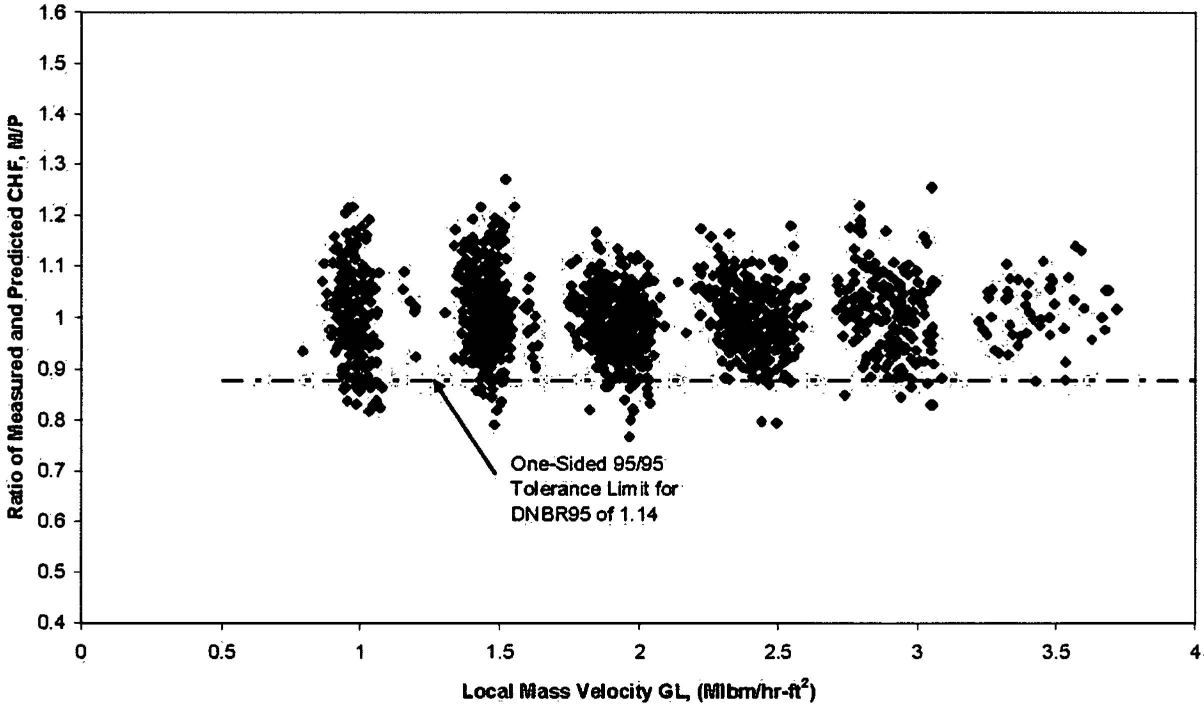

Page Intentionally Left Blank

Figure 4.2-4
Plot of M/P CHF Ratio vs. Local Quality
WNG-1 Correlation

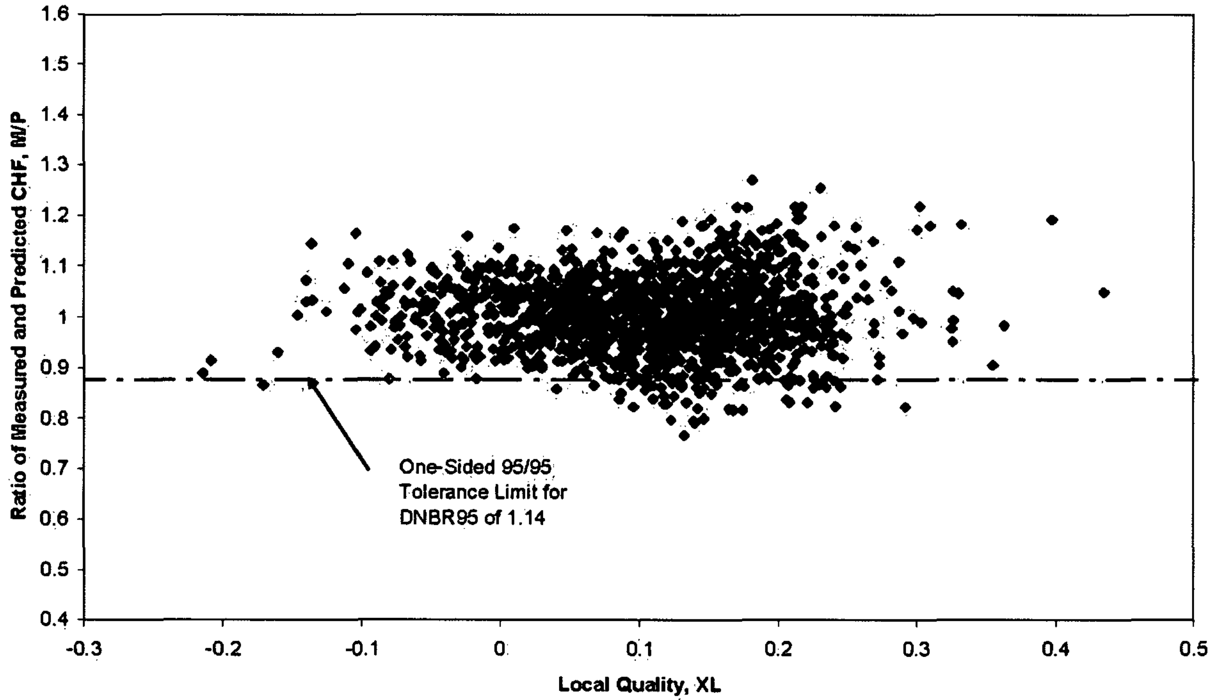

Page Intentionally Left Blank

Figure 4.2-5
Plot of M/P CHF Ratio vs. Matrix Heated Diameter, Dhm
WNG-1 Correlation

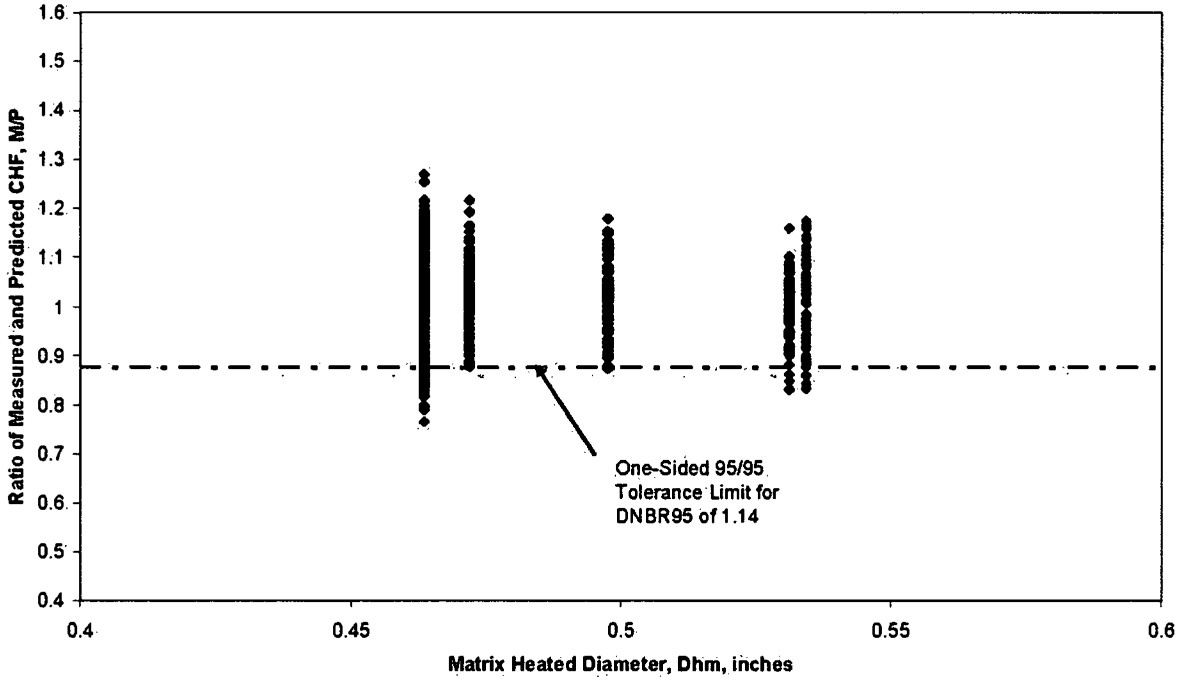

Page Intentionally Left Blank

Figure 4.2-6
Plot of M/P CHF Ratio vs. Heated Hydraulic Diameter, Dh
WNG-1 Correlation

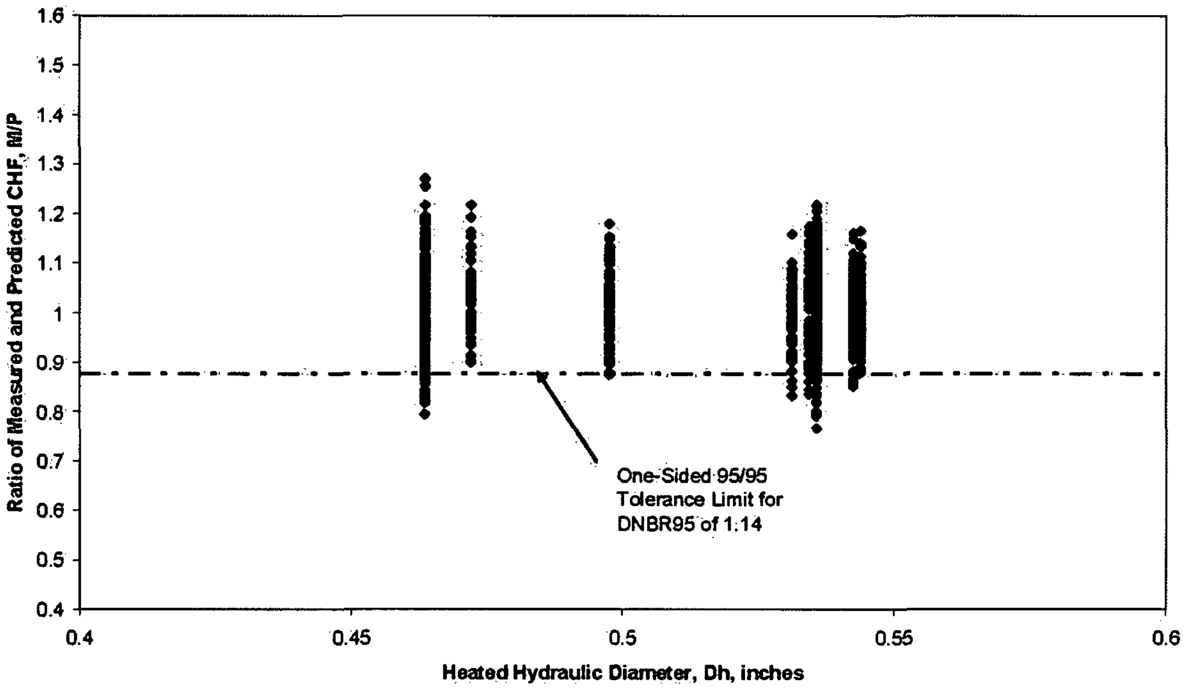

Page Intentionally Left Blank

Figure 4.2-7
Plot of M/P CHF Ratio vs. Grid Spacing Term, GST
WNG-1 Correlation

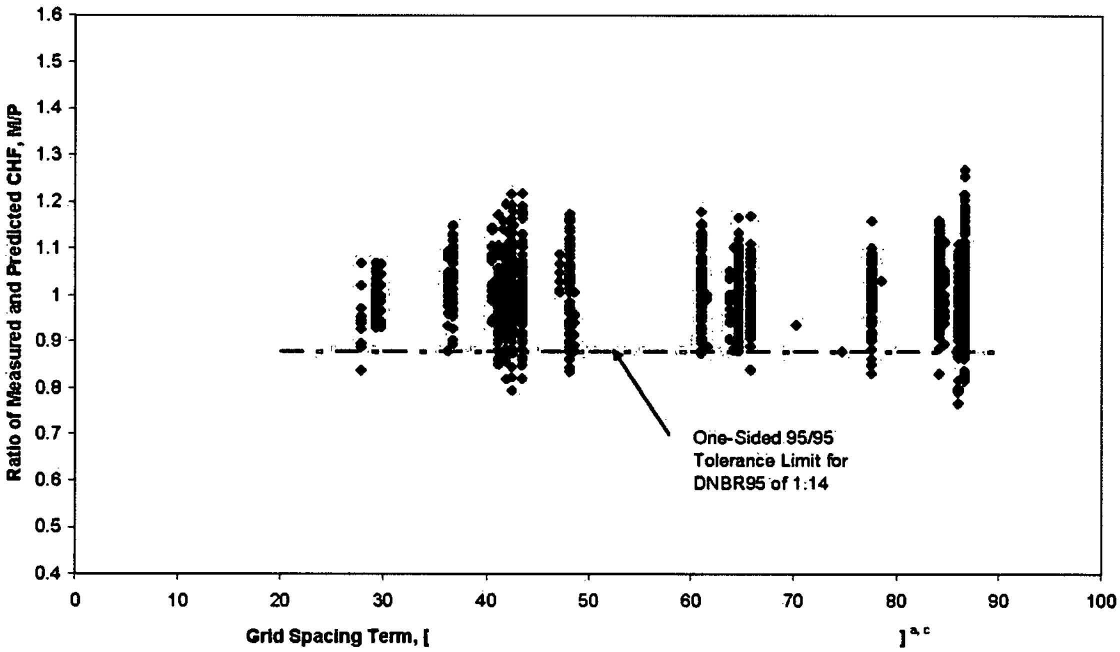

Page Intentionally Left Blank

Figure 4.2-8
Plot of M/P CHF Ratio vs. Heated Length, HL
WNG-1 Correlation

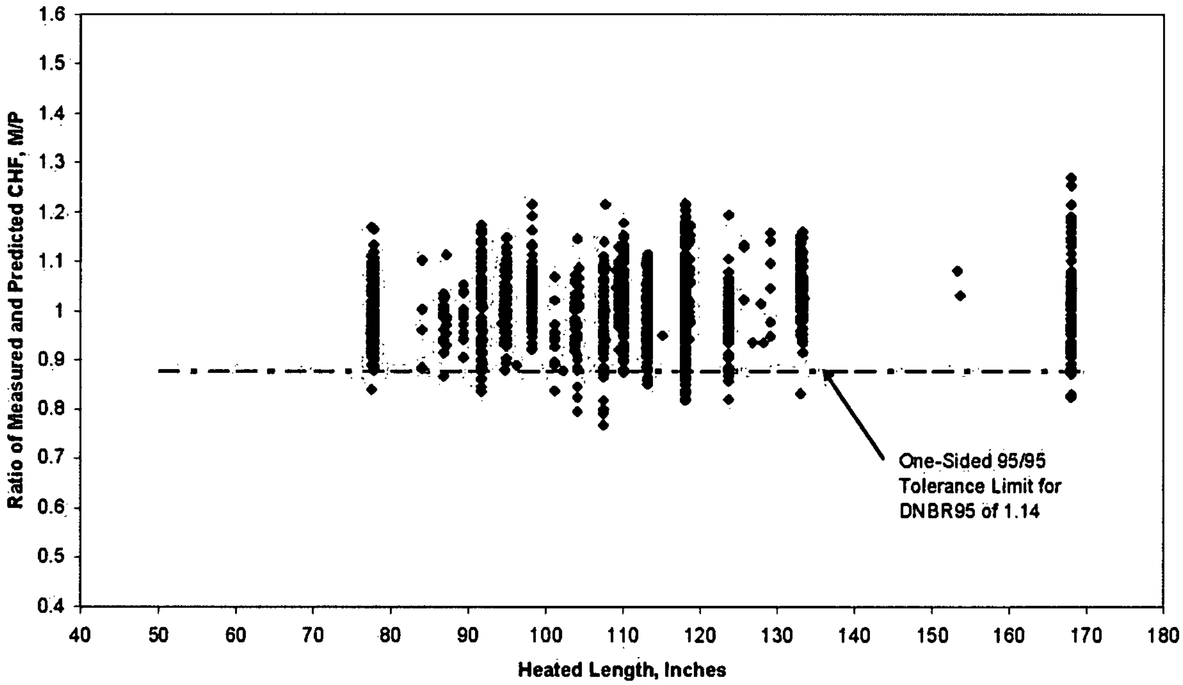

Page Intentionally Left Blank

Figure 4.2-9
Plot of M/P CHF Ratio vs. Optimized Non-Uniform Shape Factor, F_C
WNG-1 Correlation

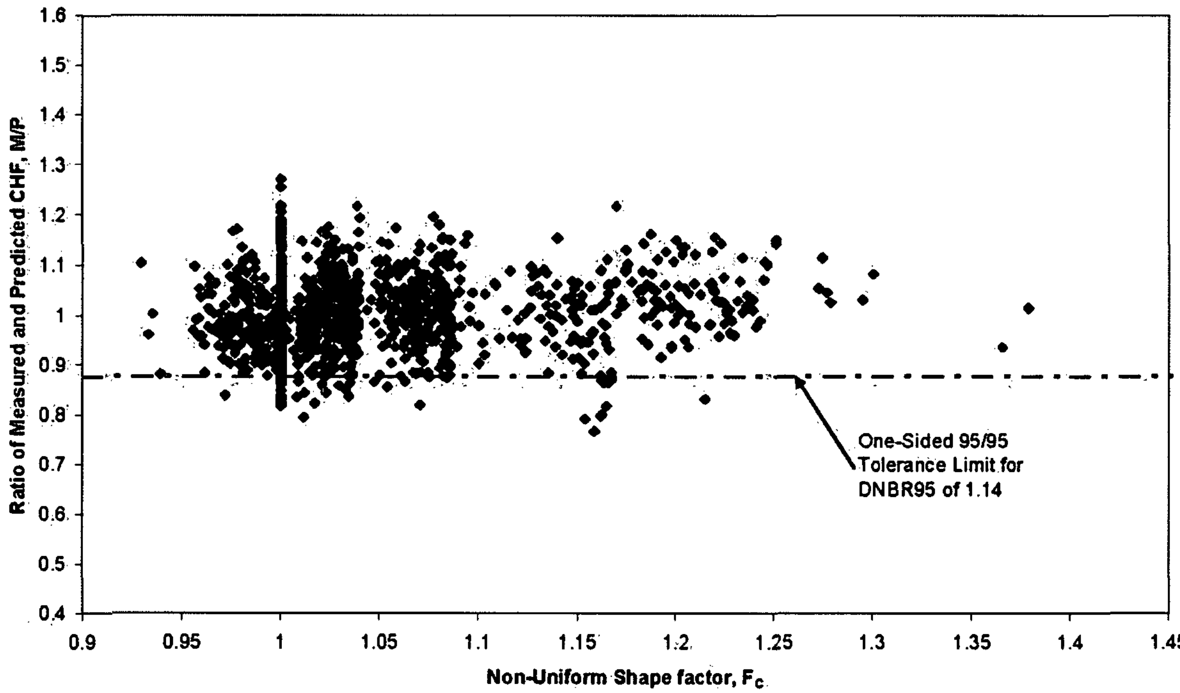

Page Intentionally Left Blank

5.0 Correlation Applications

Westinghouse intends to use the WNG-1 DNB correlation for evaluating DNB margin of the applicable Westinghouse fuel designs in plant licensing applications, in accordance with the CHF or DNB acceptance criterion defined in the Standard Review Plan (SRP), Reference 19. SRP Sections 4.2 and 4.4 state that the DNB acceptance criterion provides assurance that there be at least a 95% probability at a 95% confidence level that the hot fuel rod in the core does not experience DNB during normal operation or anticipated operational occurrence. The acceptance criterion is met in T/H design when the minimum DNBR of the hot rod in the hot channel is above the 95/95 DNBR limit of the correlation. Derivation of the WNG-1 95/95 DNBR limit was presented in the previous section. The correlation will be used only with a subchannel code that has been either used for the correlation development or qualified with its 95/95 DNBR limit in compliance with the USNRC requirements, Reference 2. Technology transfer of the WNG-1 correlation will follow through a process that meets the requirements specified in Generic Letter (GL) 83.11 Supplement 1, "Qualification for Performing Safety Analyses."

The 95/95 DNBR limit of the WNG-1 correlation with Westinghouse version of the VIPRE-01 (VIPRE) code is 1.14. The range of applicability for the WNG-1 correlation, based on its database, is summarized in Table 5-1. The WNG-1 correlation is applicable to fuel designs which are within the geometry ranges included in the correlation database. The correlation database includes the following Westinghouse fuel designs:

- 16x16 NGF design with 0.360 inch diameter fuel rods
- 17x17 NGF design with 0.374 inch diameter fuel rods
- 17x17 RFA/RFA-2 designs with 0.374 inch diameter fuel rods
- 15x15 Upgrade fuel design with 0.422 inch diameter fuel rods

The correlation application with VIPRE will be in full compliance with the conditions of the Safety Evaluation Report (SER) on the VIPRE code and modeling, Reference 2. A [

] $^{a, c}$. Additional qualification and code modification will be needed if the WNG-1 correlation is used with a subchannel code other than VIPRE.

The WNG-1 correlation implementation into reactor design applications is similar to previous implementations of other DNB correlations such as WRB-2M and ABB-NV. WNG-1 has been installed into the VIPRE code in accordance with the procedures delineated from the Westinghouse Quality Management System (QMS) (Reference 26). The WNG-1 correlation does not supersede any existing correlations, Reference 3, 6 or 7, applied for the current fuel designs.

The WNG-1 correlation will be used in DNBR calculations for core thermal limits and reactor trip setpoints and non-LOCA accident analyses. Implementation of the WNG-1 correlation will not result in any adverse impact on Westinghouse USNRC-approved methodology or licensing bases associated with the NGF or other fuel designs. The USNRC-approved methodology includes the Revised Thermal Design Procedure (RTDP) (Reference 20), the transition core evaluation method (Reference 21), the reload evaluation method (Reference 22), the fuel reconstitution evaluation method (Reference 23), three-dimensional (3D) rod ejection analysis (Reference 24) and RAVE (Reference 25). The plant analysis will account for uncertainties in plant operating parameters, nuclear and thermal parameters, and fuel fabrication parameters in addition to uncertainty in the DNB correlation.

Table 5-1
Applicable Range of WNG-1 CHF Correlation

Parameter	**Applicable Range**
Pressure (psia)	**1405 to 2495**
Local Coolant Quality	**$\leq$ 0.43**
Local Mass velocity (Mlbm/hr-ft^2)	**0.79 to 3.72**
Matrix Heated Hydraulic Diameter, Dhm (inches)	**0.46 to 0.53**
Heated Hydraulic Diameter Ratio, [ ]^{a,c}	**0.85 to 1.00**
Heated Length, HL (inches)	**48* to 168**
Grid spacing (inches)	**6.4 to 26.0**
Grid Spacing Term, GST [ ]^{a,c}	**$\geq$ 26.5****

*** Set as minimum HL value, applied at all elevations below 48 inches**
**** If Grid is in next node and GST < 26.5, set GST to 26.5**

6.0 Conclusions

The following conclusions and restrictions apply for the WNG-1 CHF correlation:

1. Analysis of the WNG-1 correlation and the source and validation data indicates the correlations accurately reflect the test results of the NGF designs (17x17 NGF, 16x16 NGF) as well as Westinghouse current designs in its database, including 17x17 RFA/RFA-2 and 15x15 Upgrade.

2. Analysis of the WNG-1 correlation and validation data indicates that a minimum DNBR limit of 1.14 for the WNG-1 correlation will provide a 95% probability with 95% confidence of not experiencing CHF on a rod showing the limiting value.

3. Statistical tests support the evaluation of the 95/95 DNBR limit of the WNG-1 correlation.

4. The WNG-1 correlation must be used in conjunction with Westinghouse version of the VIPRE-01 code (VIPRE) since the correlation was developed based on VIPRE calculated local fluid conditions.

5. The WNG-1 correlation must also be used with the Westinghouse optimized F_C shape factor for split vane designs to correct for non-uniform axial power shapes.

The range of applicability for the WNG-1 correlations is provided in Table 5-1.

Page Intentionally Left Blank

7.0 References

1. WCAP-16523-P-A, "Westinghouse Correlations WSSV and WSSV-T for Predicting Critical Heat Flux in Rod Bundles with Side-Supported Mixing Vanes," September 2007.

2. WCAP-14565-P-A, "VIPRE-01 Modeling and Qualification for Pressurized Water Reactor Non-LOCA Thermal-Hydraulic Safety Analysis," October 1999.

3. WCAP 15025-P-A, "Modified WRB-2 Correlation, WRB-2M, for Predicting Critical Heat Flux in 17x17 Rod Bundles with Modified LPD Mixing Vane Grids," April 1999.

4. CE-NPSD-785-P, "ABB-X2 Critical Heat Flux Correlation for ABB 17x17 and 16x16 Standard and Intermediate Mixing Grid Fuel," December 1994.

5. L. S. Tong, Boiling Crisis and Critical Heat Flux, U. S. Atomic Energy Commission, 1972, pp. 54-55.

6. WCAP-10444-P-A, "Reference Core Report – VANTAGE 5 Fuel Assembly," September 1985.

7. WCAP-8762-P-A, "New Westinghouse Correlation WRB-1 for Predicting Critical Heat Flux in Rod Bundles with Mixing Vane Grids," July 1984.

8. CENPD-387-P-A, Rev.00, "ABB Critical Heat Flux Correlations for PWR Fuel," May 2000.

9. CENPD-162-P-A, "C-E Critical Heat Flux," September 1976.

10. EPRI NP-2609, "Parametric Study of CHF Data Volume 3, Part 1: Critical Heat Flux Data," September 1982.

11. CE-NPSD-718-P, "Mixing Data Evaluation for ABB Critical Heat Flux Tests 82 to 88," March 1992.

12. Experimental Statistics, National Bureau of Standards Handbook 91, Department of Commerce, August 1963.

13. ANSI N15.15-1974, "American National Standard Assessment of the Assumption of Normality (Employing Individual Observed Values)," October 1973.

14. Crow, E. L., Davis, F. A., and Maxfield, M. W., Statistics Manual, Dover Publications, Inc., 1960, Chapters 3 and 4.

15. Scheafer and McClave, "Probability and Statistics for Engineers, 3 ed," PWS-KENT, 1990.

16. Owens, D. B., "Factors for One-Sided Tolerance Limits and for Variable Sampling Plans," SC-R-607, Sandia Corporation, March 1963.

17. Pearson, E. S., and Hartley, H. O., Biometrika Tables for Statisticians, Vol. I, 3rd Edition, Cambridge University Press, 1966, pp. 63-66 and Table 7.

18. Siegal, S., and Castellan, Jr., N. J., Non-parametric Statistics for the Behavioral Sciences, 2nd Edition, 1988, McGraw-Hill, pp. 128-137 & 206-216.

19. NUREG-0800, "U.S. Nuclear Regulatory Commission Office of Nuclear Reactor Regulation Standard Review Plan Section 4.2, 'Fuel System Design' and Section 4.4, 'Thermal and Hydraulic Design'," Revision 2, July 1981.

20. WCAP-11397-P-A, "Revised Thermal Design Procedure," April 1989.

21. WCAP-11837-P-A, "Extension of Methodology for Calculating Transition Core DNBR Penalties," January 1990.

22. WCAP-9272-P-A, "Westinghouse Reload Safety Evaluation Methodology," July 1985.

23. WCAP-13060-P-A, "Westinghouse Fuel Reconstitution Evaluation Methodology," January 1993.

24. WCAP-15806-P-A, "Westinghouse Control Rod Ejection Accident Analysis Methodology Using Multi-Dimensional Kinetics," October 2003.

25. WCAP-16259-P-A, "Westinghouse Methodology for Application of 3-D Transient Neutronics to Non-LOCA Accident Analysis," August 2006.

26. "Westinghouse Electric Company Quality Management System (QMS)," Revision 5, 2002.

Appendix A
WNG-1 VIPRE Database

Page Intentionally Left Blank

Appendix A: WNG-1 VIPRE Database

A detailed summary of the WNG-1 Correlation Database is shown in Table A-1 and the Validation Database is shown in Table A-2. The tables in this appendix summarize the raw data from Columbia data files, the test geometry information needed for the correlation development, the predicted local coolant conditions taken from the VIPRE runs. The tabulation presented here gives the data from all CHF experiments with test sections described in Table 2-1. Repeat runs in the correlation database and runs with only cold rods indicating DNB, identified in bold italics, were eliminated in the final correlation database along with points outside the correlation parameter limits. Nomenclature for heading abbreviations in Appendix A are defined below:

TS = Test Section Number
TD = Test Section Type (UM is Uniform Shape without Guide Thimble, UT is Uniform Shape with Guide Thimble, NM is Non-Uniform Shape without Guide Thimble , and NT is Non-Uniform Shape with Guide Thimble)
Press = Test Section Pressure (psia)
Tin = Test Section Inlet Temperature (°F)
Gavg = Average Test Section Mass Velocity (Mlbm/hr-ft^2)
Qavg = Test Section Critical Bundle Average Heat Flux (MBtu/hr-ft^2)
DROD = Primary DNB Rod Thermocouple Number
DCH = VIPRE Subchannel Number Where Local Coolant Conditions are Selected
GL = Local Mass Velocity in CHF Channel (Mlbm/hr-ft^2)
XL = Local Quality in CHF Channel (fraction)
CHFm = Measured CHF (MBtu/hr-ft^2)
F_C = Non-uniform Shape Factor = 1.00 for Uniform Axial Power Shape
Based on Optimized F_C for Non-uniform Axial Power Shape
GS = Nominal Upstream Grid Spacing from [ ]$^{a, c}$ (in)
HL = Heated Length to CHF Site (in)
DG = Distance from [ ]$^{a, c}$ Grid to CHF Site (in)
De = Wetted Hydraulic Diameter of CHF Channel (in)
Dh = Heated Hydraulic Diameter of CHF Channel (in)
Dhm = Heated Hydraulic Diameter of Matrix Channel (in)

Page Intentionally Left Blank

Table A-1
WNG-1 Correlation Database

a, b, c

TS TD	Run	Press.	Tin	Gavg	Qavg	DROD	DCH	GL	XL	CHFm	FC	GS	HL	DG	De	Dh	Dhm

Table A-1 (Continued)
WNG-1 Correlation Database

a, b, c

TS TD	Run	Press.	Tin	Gavg	Qavg	DROD	DCH	GL	XL	CHFm	FC	GS	HL	DG	De	Dh	Dhm

Table A-1 (Continued)
WNG-1 Correlation Database

a, b, c

TS TD	Run	Press.	Tin	Gavg	Qavg	DROD	DCH	GL	XL	CHFm	FC	GS	HL	DG	De	Dh	Dhm

Table A-1 (Continued)
WNG-1 Correlation Database

a, b, c

TS TD	Run	Press.	Tin	Gavg	Qavg	DROD	DCH	GL	XL	CHFm	FC	GS	HL	DG	De	Dh	Dhm

Table A-1 (Continued)
WNG-1 Correlation Database

a, b, c

TS TD	Run	Press.	Tin	Gavg	Qavg	DROD	DCH	GL	XL	CHFm	FC	GS	HL	DG	De	Dh	Dhm

Table A-1 (Continued)
WNG-1 Correlation Database

a, b, c

TS TD	Run	Press.	Tin	Gavg	Qavg	DROD	DCH	GL	XL	CHFm	FC	GS	HL	DG	De	Dh	Dhm

Table A-1 (Continued)
WNG-1 Correlation Database

a, b, c

TS TD	Run	Press.	Tin	Gavg	Qavg	DROD	DCH	GL	XL	CHFm	FC	GS	HL	DG	De	Dh	Dhm

Table A-1 (Continued)
WNG-1 Correlation Database

a, b, c

TS TD	Run	Press.	Tin	Gavg	Qavg	DROD	DCH	GL	XL	CHFm	FC	GS	HL	DG	De	Dh	Dhm

Table A-1 (Continued)
WNG-1 Correlation Database

a, b, c

TS TD	Run	Press.	Tin	Gavg	Qavg	DROD	DCH	GL	XL	CHFm	FC	GS	HL	DG	De	Dh	Dhm

Table A-1 (Continued)
WNG-1 Correlation Database

a, b, c

TS TD	Run	Press.	Tin	Gavg	Qavg	DROD	DCH	GL	XL	CHFm	FC	GS	HL	DG	De	Dh	Dhm

Table A-1 (Continued)
WNG-1 Correlation Database

a, b, c

TS TD	Run	Press.	Tin	Gavg	Qavg	DROD	DCH	GL	XL	CHFm	FC	GS	HL	DG	De	Dh	Dhm

Table A-1 (Continued)
WNG-1 Correlation Database

a, b, c

TS TD	Run	Press.	Tin	Gavg	Qavg	DROD	DCH	GL	XL	CHFm	FC	GS	HL	DG	De	Dh	Dhm

Table A-1 (Continued)
WNG-1 Correlation Database

a, b, c

TS TD	Run	Press.	Tin	Gavg	Qavg	DROD	DCH	GL	XL	CHFm	FC	GS	HL	DG	De	Dh	Dhm

Table A-1 (Continued)
WNG-1 Correlation Database

a, b, c

TS TD	Run	Press.	Tin	Gavg	Qavg	DROD	DCH	GL	XL	CHFm	FC	GS	HL	DG	De	Dh	Dhm

Table A-1 (Continued)
WNG-1 Correlation Database

a, b, c

TS TD	Run	Press.	Tin	Gavg	Qavg	DROD	DCH	GL	XL	CHFm	FC	GS	HL	DG	De	Dh	Dhm

Table A-1 (Continued)
WNG-1 Correlation Database

a, b, c

TS TD	Run	Press.	Tin	Gavg	Qavg	DROD	DCH	GL	XL	CHFm	FC	GS	HL	DG	De	Dh	Dhm

Table A-1 (Continued)
WNG-1 Correlation Database

a, b, c

TS TD	Run	Press.	Tin	Gavg	Qavg	DROD	DCH	GL	XL	CHFm	FC	GS	HL	DG	De	Dh	Dhm

Table A-1 (Continued)
WNG-1 Correlation Database

a, b, c

TS.TD	Run	Press.	Tin	Gavg	Qavg	DROD	DCH	GL	XL	CHFm	FC	GS	HL	DG	De	Dh	Dhm

Table A-1 (Continued)
WNG-1 Correlation Database

a, b, c

TS TD	Run	Press.	Tin	Gavg	Qavg	DROD	DCH	GL	XL	CHFm	FC	GS	HL	DG	De	Dh	Dhm

Table A-1 (Continued)
WNG-1 Correlation Database

a, b, c

TS TD	Run	Press.	Tin	Gavg	Qavg	DROD	DCH	GL	XL	CHFm	FC	GS	HL	DG	De	Dh	Dhm

Table A-1 (Continued)
WNG-1 Correlation Database

a, b, c

TS TD	Run	Press.	Tin	Gavg	Qavg	DROD	DCH	GL	XL	CHFm	FC	GS	HL	DG	De	Dh	Dhm

Table A-1 (Continued)
WNG-1 Correlation Database

a, b, c

TS TD	Run	Press.	Tin	Gavg	Qavg	DROD	DCH	GL	XL	CHFm	FC	GS	HL	DG	De	Dh	Dhm

Table A-1 (Continued)
WNG-1 Correlation Database

a, b, c

TS TD	Run	Press.	Tin	Gavg	Qavg	DROD	DCH	GL	XL	CHFm	FC	GS	HL	DG	De	Dh	Dhm

Table A-1 (Continued)
WNG-1 Correlation Database

a, b, c

TS TD	Run	Press.	Tin	Gavg	Qavg	DROD	DCH	GL	XL	CHFm	FC	GS	HL	DG	De	Dh	Dhm

Table A-1 (Continued)
WNG-1 Correlation Database

a, b, c

TS TD	Run	Press.	Tin	Gavg	Qavg	DROD	DCH	GL	XL	CHFm	FC	GS	HL	DG	De	Dh	Dhm

Table A-1 (Continued)
WNG-1 Correlation Database

a, b, c

TS TD	Run	Press.	Tin	Gavg	Qavg	DROD	DCH	GL	XL	CHFm	FC	GS	HL	DG	De	Dh	Dhm

Table A-1 (Continued)
WNG-1 Correlation Database

a, b, c

TS TD	Run	Press.	Tin	Gavg	Qavg	DROD	DCH	GL	XL	CHFm	FC	GS	HL	DG	De	Dh	Dhm

Table A-1 (Continued)
WNG-1 Correlation Database

a, b, c

TS TD	Run	Press.	Tin	Gavg	Qavg	DROD	DCH	GL	XL	CHFm	FC	GS	HL	DG	De	Dh	Dhm

Table A-1 (Continued)
WNG-1 Correlation Database

a, b, c

TS TD	Run	Press.	Tin	Gavg	Qavg	DROD	DCH	GL	XL	CHFm	FC	GS	HL	DG	De	Dh	Dhm

Table A-1 (Continued)
WNG-1 Correlation Database

a, b, c

TS TD	Run	Press.	Tin	Gavg	Qavg	DROD	DCH	GL	XL	CHFm	FC	GS	HL	DG	De	Dh	Dhm

Table A-1 (Continued)
WNG-1 Correlation Database

a, b, c

TS TD	Run	Press.	Tin	Gavg	Qavg	DROD	DCH	GL	XL	CHFm	FC	GS	HL	DG	De	Dh	Dhm

Table A-1 (Continued)
WNG-1 Correlation Database

a, b, c

TS TD	Run	Press.	Tin	Gavg	Qavg	DROD	DCH	GL	XL	CHFm	FC	GS	HL	DG	De	Dh	Dhm

Table A-1 (Continued)
WNG-1 Correlation Database

a, b, c

TS TD	Run	Press.	Tin	Gavg	Qavg	DROD	DCH	GL	XL	CHFm	FC	GS	HL	DG	De	Dh	Dhm

Table A-1 (Continued)
WNG-1 Correlation Database

a, b, c

TS TD	Run	Press.	Tin	Gavg	Qavg	DROD	DCH	GL	XL	CHFm	FC	GS	HL	DG	De	Dh	Dhm

Table A-1 (Continued)
WNG-1 Correlation Database

a, b, c

TS TD	Run	Press.	Tin	Gavg	Qavg	DROD	DCH	GL	XL	CHFm	FC	GS	HL	DG	De	Dh	Dhm

Table A-1 (Continued)
WNG-1 Correlation Database

a, b, c

TS	TD	Run	Press.	Tin	Gavg	Qavg	DROD	DCH	GL	XL	CHFm	FC	GS	HL	DG	De	Dh	Dhm

Table A-1 (Continued)
WNG-1 Correlation Database

a, b, c

TS TD	Run	Press.	Tin	Gavg	Qavg	DROD	DCH	GL	XL	CHFm	FC	GS	HL	DG	De	Dh	Dhm

Table A-1 (Continued)
WNG-1 Correlation Database

a, b, c

TS TD	Run	Press.	Tin	Gavg	Qavg	DROD	DCH	GL	XL	CHFm	FC	GS	HL	DG	De	Dh	Dhm

Table A-1 (Continued)
WNG-1 Correlation Database

a, b, c

TS TD	Run	Press.	Tin	Gavg	Qavg	DROD	DCH	GL	XL	CHFm	FC	GS	HL	DG	De	Dh	Dhm

Table A-1 (Continued)
WNG-1 Correlation Database

a, b, c

TS TD	Run	Press.	Tin	Gavg	Qavg	DROD	DCH	GL	XL	CHFm	FC	GS	HL	DG	De	Dh	Dhm

Table A-1 (Continued)
WNG-1 Correlation Database

a, b, c

TS.TD	Run	Press.	Tin	Gavg	Qavg	DROD	DCH	GL	XL	CHFm	FC	GS	HL	DG	De	Dh	Dhm

Table A-2
WNG-1 Validation Database

a, b, c

TS TD	Run	Press.	Tin	Gavg	Qavg	DROD	DCH	GL	XL	CHFm	FC	GS	HL	DG	De	Dh	Dhm

Table A-2 (Continued)
WNG-1 Validation Database

a, b, c

TS TD	Run	Press.	Tin	Gavg	Qavg	DROD	DCH	GL	XL	CHFm	FC	GS	HL	DG	De	Dh	Dhm

Table A-2 (Continued)
WNG-1 Validation Database

a, b, c

TS TD	Run	Press.	Tin	Gavg	Qavg	DROD	DCH	GL	XL	CHFm	FC	GS	HL	DG	De	Dh	Dhm

Table A-2 (Continued)
WNG-1 Validation Database

a, b, c

TS TD	Run	Press.	Tin	Gavg	Qavg	DROD	DCH	GL	XL	CHFm	FC	GS	HL	DG	De	Dh	Dhm

Table A-2 (Continued)
WNG-1 Validation Database

a, b, c

TS TD	Run	Press.	Tin	Gavg	Qavg	DROD	DCH	GL	XL	CHFm	FC	GS	HL	DG	De	Dh	Dhm

Table A-2 (Continued)
WNG-1 Validation Database

a, b, c

TS TD	Run	Press.	Tin	Gavg	Qavg	DROD	DCH	GL	XL	CHFm	FC	GS	HL	DG	De	Dh	Dhm

Table A-2 (Continued)
WNG-1 Validation Database

a, b, c

TS TD	Run	Press.	Tin	Gavg	Qavg	DROD	DCH	GL	XL	CHFm	FC	GS	HL	DG	De	Dh	Dhm

Table A-2 (Continued)
WNG-1 Validation Database

a, b, c

TS TD	Run	Press.	Tin	Gavg	Qavg	DROD	DCH	GL	XL	CHFm	FC	GS	HL	DG	De	Dh	Dhm

Table A-2 (Continued)
WNG-1 Validation Database

a, b, c

TS TD	Run	Press.	Tin	Gavg	Qavg	DROD	DCH	GL	XL	CHFm	FC	GS	HL	DG	De	Dh	Dhm

Table A-2 (Continued)
WNG-1 Validation Database

a, b, c

TS TD	Run	Press.	Tin	Gavg	Qavg	DROD	DCH	GL	XL	CHFm	FC	GS	HL	DG	De	Dh	Dhm

Table A-2 (Continued)
WNG-1 Validation Database

a, b, c

TS TD	Run	Press.	Tin	Gavg	Qavg	DROD	DCH	GL	XL	CHFm	FC	GS	HL	DG	De	Dh	Dhm

Table A-2 (Continued)
WNG-1 Validation Database

a, b, c

TS TD	Run	Press.	Tin	Gavg	Qavg	DROD	DCH	GL	XL	CHFm	FC	GS	HL	DG	De	Dh	Dhm

Table A-2 (Continued)
WNG-1 Validation Database

a, b, c

TS TD	Run	Press.	Tin	Gavg	Qavg	DROD	DCH	GL	XL	CHFm	FC	GS	HL	DG	De	Dh	Dhm

Appendix B
WNG-1 VIPRE Statistical Output

Page Intentionally Left Blank

Appendix B: WNG-1 VIPRE Statistical Output

A detailed summary of the statistical output of the WNG-1 correlation database is given in Table B-1. A detailed summary of the statistical output of the WNG-1 validation database is given in Table B-2. For each test run in Tables B-1 and B-2, the values for the correlation variables, the measured CHF and WNG-1 predicted CHF are given, along with the value for the M/P CHF ratio. The repeat test runs and any test runs with variables outside the correlation parameter range are removed from Tables B-1 and B-2. The individual test section and overall database statistics are given at the end of the output in Tables B-1 and B-2. The individual test and final combined database statistics are given in Table B-3 for the database used to determine the 95/95 DNBR limit. The database consisted of the correlation database and validation tests for current grids that increased the correlation parameter range. The statistics for the subsets based on test, rod and strap geometries are also given in Table B-3. Nomenclature for heading abbreviations in Appendix B is defined below:

TS = Test Section Number
TD = Test Section Type (UM is Uniform Shape without Guide Thimble, UT is Uniform Shape with Guide Thimble, NM IS Non-Uniform Shape without Guide Thimble, NT is Non-Uniform Shape with Guide Thimble)
Press = Test Section Pressure (psia)
GL = Local Mass Velocity in CHF Channel (Mlbm/hr-ft^2)
XL = Local Quality in CHF Channel (fraction)
F_C = Non-uniform Shape Factor = 1.00 for Uniform Axial Power Shape Based on optimized F_C for Non-uniform Axial Power Shape
GS = Upstream Nominal Grid Spacing, [ ]^{a,c}
HL = Heated Length to CHF Site (in)
DG = Distance from [ ]^{a,c} Grid to CHF Site (in)
Dh = Heated Hydraulic Diameter of CHF Channel (in)
Dhm = Heated Hydraulic Diameter of Matrix Channel (in)
GST = Grid Spacing Term, [ ]^{a,c}
CHFM = Measured CHF (MBtu/hr-ft^2)
CHFP = WNG-1 Predicted CHF divided by F_C (MBtu/hr-ft^2)

Page Intentionally Left Blank

Table B-1
Statistical Output of WNG-1 Correlation Database

a, b, c

TS TD	Run	Press.	GL	XL	FC	GS	HL	DG	Dh	Dhm	GST	CHFm	CHFp	M/P-1	M/P

Table B-1 (Continued)
Statistical Output of WNG-1 Correlation Database

a, b, c

TS TD	Run	Press.	GL	XL	FC	GS	HL	DG	Dh	Dhm	GST	CHFm	CHFp	M/P-1	M/P

Table B-1 (Continued)
Statistical Output of WNG-1 Correlation Database

a, b, c

TS TD	Run	Press.	GL	XL	FC	GS	HL	DG	Dh	Dhm	GST	CHFm	CHFp	M/P-1	M/P

Table B-1 (Continued)
Statistical Output of WNG-1 Correlation Database

a, b, c

TS TD	Run	Press.	GL	XL	FC	GS	HL	DG	Dh	Dhm	GST	CHFm	CHFp	M/P-1	M/P

Table B-1 (Continued)
Statistical Output of WNG-1 Correlation Database

a, b, c

TS TD	Run	Press.	GL	XL	FC	GS	HL	DG	Dh	Dhm	GST	CHFm	CHFp	M/P-1	M/P

Table B-1 (Continued)
Statistical Output of WNG-1 Correlation Database

a, b, c

TS TD	Run	Press.	GL	XL	FC	GS	HL	DG	Dh	Dhm	GST	CHFm	CHFp	M/P-1	M/P

Table B-1 (Continued)
Statistical Output of WNG-1 Correlation Database

a, b, c

TS TD	Run	Press.	GL	XL	FC	GS	HL	DG	Dh	Dhm	GST	CHFm	CHFp	M/P-1	M/P

Table B-1 (Continued)
Statistical Output of WNG-1 Correlation Database

a, b, c

TS TD	Run	Press.	GL	XL	FC	GS	HL	DG	Dh	Dhm	GST	CHFm	CHFp	M/P-1	M/P

Table B-1 (Continued)
Statistical Output of WNG-1 Correlation Database

a, b, c

TS TD	Run	Press.	GL	XL	FC	GS	HL	DG	Dh	Dhm	GST	CHFm	CHFp	M/P-1	M/P

Table B-1 (Continued)
Statistical Output of WNG-1 Correlation Database

a, b, c

TS TD	Run	Press.	GL	XL	FC	GS	HL	DG	Dh	Dhm	GST	CHFm	CHFp	M/P-1	M/P

Table B-1 (Continued)
Statistical Output of WNG-1 Correlation Database

a, b, c

TS TD	Run	Press.	GL	XL	FC	GS	HL	DG	Dh	Dhm	GST	CHFm	CHFp	M/P-1	M/P

Table B-1 (Continued)
Statistical Output of WNG-1 Correlation Database

a, b, c

TS TD	Run	Press.	GL	XL	FC	GS	HL	DG	Dh	Dhm	GST	CHFm	CHFp	M/P-1	M/P

Table B-1 (Continued)
Statistical Output of WNG-1 Correlation Database

TS TD	Run	Press.	GL	XL	FC	GS	HL	DG	Dh	Dhm	GST	CHFm	CHFp	M/P-1	M/P

a, b, c

Table B-1 (Continued)
Statistical Output of WNG-1 Correlation Database

a, b, c

TS TD	Run	Press.	GL	XL	FC	GS	HL	DG	Dh	Dhm	GST	CHFm	CHFp	M/P-1	M/P

Table B-1 (Continued)
Statistical Output of WNG-1 Correlation Database

a, b, c

TS TD	Run	Press.	GL	XL	FC	GS	HL	DG	Dh	Dhm	GST	CHFm	CHFp	M/P-1	M/P

Table B-1 (Continued)
Statistical Output of WNG-1 Correlation Database

a, b, c

TS TD	Run	Press.	GL	XL	FC	GS	HL	DG	Dh	Dhm	GST	CHFm	CHFp	M/P-1	M/P

Table B-1 (Continued)
Statistical Output of WNG-1 Correlation Database

a, b, c

TS TD	Run	Press.	GL	XL	FC	GS	HL	DG	Dh	Dhm	GST	CHFm	CHFp	M/P-1	M/P

Table B-1 (Continued)
Statistical Output of WNG-1 Correlation Database

a, b, c

TS TD	Run	Press.	GL	XL	FC	GS	HL	DG	Dh	Dhm	GST	CHFm	CHFp	M/P-1	M/P

Table B-1 (Continued)
Statistical Output of WNG-1 Correlation Database

a, b, c

TS TD	Run	Press.	GL	XL	FC	GS	HL	DG	Dh	Dhm	GST	CHFm	CHFp	M/P-1	M/P

Table B-1 (Continued)
Statistical Output of WNG-1 Correlation Database

a, b, c

TS TD	Run	Press.	GL	XL	FC	GS	HL	DG	Dh	Dhm	GST	CHFm	CHFp	M/P-1	M/P

Table B-1 (Continued)
Statistical Output of WNG-1 Correlation Database

a, b, c

TS TD	Run	Press.	GL	XL	FC	GS	HL	DG	Dh	Dhm	GST	CHFm	CHFp	M/P-1	M/P

Table B-1 (Continued)
Statistical Output of WNG-1 Correlation Database

a, b, c

TS TD	Run	Press.	GL	XL	FC	GS	HL	DG	Dh	Dhm	GST	CHFm	CHFp	M/P-1	M/P

Table B-1 (Continued)
Statistical Output of WNG-1 Correlation Database

a, b, c

TS TD	Run	Press.	GL	XL	FC	GS	HL	DG	Dh	Dhm	GST	CHFm	CHFp	M/P-1	M/P

Table B-1 (Continued)
Statistical Output of WNG-1 Correlation Database

a, b, c

TS TD	Run	Press.	GL	XL	FC	GS	HL	DG	Dh	Dhm	GST	CHFm	CHFp	M/P-1	M/P

Table B-1 (Continued)
Statistical Output of WNG-1 Correlation Database

a, b, c

TS TD	Run	Press.	GL	XL	FC	GS	HL	DG	Dh	Dhm	GST	CHFm	CHFp	M/P-1	M/P

Table B-1 (Continued)
Statistical Output of WNG-1 Correlation Database

a, b, c

TS TD	Run	Press.	GL	XL	FC	GS	HL	DG	Dh	Dhm	GST	CHFm	CHFp	M/P-1	M/P

Table B-1 (Continued)
Statistical Output of WNG-1 Correlation Database

a, b, c

TS TD	Run	Press.	GL	XL	FC	GS	HL	DG	Dh	Dhm	GST	CHFm	CHFp	M/P-1	M/P

Table B-1 (Continued)
Statistical Output of WNG-1 Correlation Database

a, b, c

TS TD	Run	Press.	GL	XL	FC	GS	HL	DG	Dh	Dhm	GST	CHFm	CHFp	M/P-1	M/P

Table B-1 (Continued)
Statistical Output of WNG-1 Correlation Database

a, b, c

TS TD	Run	Press.	GL	XL	FC	GS	HL	DG	Dh	Dhm	GST	CHFm	CHFp	M/P-1	M/P

Table B-1 (Continued)
Statistical Output of WNG-1 Correlation Database

a, b, c

TS TD	Run	Press.	GL	XL	FC	GS	HL	DG	Dh	Dhm	GST	CHFm	CHFp	M/P-1	M/P

Table B-1 (Continued)
Statistical Output of WNG-1 Correlation Database

a, b, c

TS TD	Run	Press.	GL	XL	FC	GS	HL	DG	Dh	Dhm	GST	CHFm	CHFp	M/P-1	M/P

Table B-1 (Continued)
Statistical Output of WNG-1 Correlation Database

Correlation Data

a, b, c

Table B-2
Statistical Output of WNG-1 Validation Database

a, b, c

TS TD	Run	Press.	GL	XL	FC	GS	HL	DG	Dh	Dhm	GST	CHFm	CHFp	M/P-1	M/P

Table B-2 (Continued)
Statistical Output of WNG-1 Validation Database

a, b, c

TS TD	Run	Press.	GL	XL	FC	GS	HL	DG	Dh	Dhm	GST	CHFm	CHFp	M/P-1	M/P

Table B-2 (Continued)
Statistical Output of WNG-1 Validation Database

a, b, c

TS TD	Run	Press.	GL	XL	FC	GS	HL	DG	Dh	Dhm	GST	CHFm	CHFp	M/P-1	M/P

Table B-2 (Continued)
Statistical Output of WNG-1 Validation Database

a, b, c

TS TD	Run	Press.	GL	XL	FC	GS	HL	DG	Dh	Dhm	GST	CHFm	CHFp	M/P-1	M/P

Table B-2 (Continued)
Statistical Output of WNG-1 Validation Database

a, b, c

TS TD	Run	Press.	GL	XL	FC	GS	HL	DG	Dh	Dhm	GST	CHFm	CHFp	M/P-1	M/P

Table B-2 (Continued)
Statistical Output of WNG-1 Validation Database

a, b, c

TS TD	Run	Press.	GL	XL	FC	GS	HL	DG	Dh	Dhm	GST	CHFm	CHFp	M/P-1	M/P

Table B-2 (Continued)
Statistical Output of WNG-1 Validation Database

a, b, c

TS TD	Run	Press.	GL	XL	FC	GS	HL	DG	Dh	Dhm	GST	CHFm	CHFp	M/P-1	M/P

Table B-2 (Continued)
Statistical Output of WNG-1 Validation Database

a, b, c

TS TD	Run	Press.	GL	XL	FC	GS	HL	DG	Dh	Dhm	GST	CHFm	CHFp	M/P-1	M/P

Table B-2 Continued
Statistical Output of WNG-1 Validation Database

a, b, c

TS	TD	Run	Press.	GL	XL	FC	GS	HL	DG	Dh	Dhm	GST	CHFm	CHFp	M/P-1	M/P

Table B-2 (Continued)
Statistical Output of WNG-1 Validation Database

Validataion Data

a, b, c

Table B-3
Statistical Output of WNG-1 Combined Database for DNBR95 Limit

<u>Combined Data</u>

a, b, c

Page Intentionally Left Blank

Appendix C
WNG-1 CHF Test Geometries

Page Intentionally Left Blank

Appendix C: WNG-1 CHF Test Geometries

The test section radial and axial geometries for the tests used in the development and validation of the WNG-1 correlation are shown in Figures C-1 through C-37. The axial relative power input into the VIPRE code for the non-uniform tests in the correlation database is shown in Table C-1. The axial relative power input into the VIPRE code for the non-uniform tests in the validation database is shown in Table C-2.

Page Intentionally Left Blank

Table C-1

VIPRE Axial Power Distribution Input for Correlation Tests

a, b, c

Table C-2
VIPRE Axial Power Distribution Inputs for Correlation Tests

a, b, c

Figure C-1
RADIAL GEOMETRY – CHF TEST SECTION 82

a, b, c

[ ]

Figure C-2
AXIAL GEOMETRY – CHF TEST SECTIONS 82 , 83 and 94

a, b, c

[ ]

Figure C-3

RADIAL GEOMETRY – CHF TEST SECTION 94

a, b, c

Figure C-4
RADIAL GEOMETRY – CHF TEST SECTION 85-1
First 82 CHF Points

a, b, c

[ ]

Figure C-5
RADIAL GEOMETRY – CHF TEST SECTION 85-2
Last 24 CHF Points

a, b, c

Figure C-6
AXIAL GEOMETRY – CHF TEST SECTION 85

a, b, c

[ ]

Figure C-7
RADIAL GEOMETRY – CHF TEST SECTION 87

a, b, c

Figure C-8
AXIAL GEOMETRY – CHF TEST SECTION 87

a, b, c

Figure C-9
RADIAL GEOMETRY – CHF TEST SECTION 89

a, b, c

[ ]

Figure C-10
AXIAL GEOMETRY – CHF TEST SECTION 89

a, b, c

Figure C-11
RADIAL GEOMETRY – CHF TEST SECTION 104

a, b, c

[ ]

Figure C-12
AXIAL GEOMETRY – CHF TEST SECTIONS 104 and 105

a, b, c

Figure C-13

RADIAL GEOMETRY – CHF TEST SECTION 105

a, b, c

[ ]

Figure C-14
RADIAL GEOMETRY – CHF TEST SECTION 90

a, b, c

Figure C-15
AXIAL GEOMETRY – CHF TEST SECTION 90

a, b, c

Figure C-16
RADIAL GEOMETRY – CHF TEST SECTION 96

a, b, c

Figure C-17
AXIAL GEOMETRY – CHF TEST SECTIONS 96, 97 and 103

a, b, c

Figure C-18
RADIAL GEOMETRY – CHF TEST SECTION 97

a, b, c

Figure C-19
RADIAL GEOMETRY – CHF TEST SECTION 98

a, b, c

Figure C-20
AXIAL GEOMETRY – CHF TEST SECTIONS 98 and 99

a, b, c

[ ]

Figure C-21

RADIAL GEOMETRY – CHF TEST SECTION 99

a, b, c

Figure C-22
RADIAL GEOMETRY – CHF TEST SECTION 95

a, b, c

Figure C-23
AXIAL GEOMETRY – CHF TEST SECTION 95

a, b, c

Figure C-24
RADIAL GEOMETRY – CHF TEST SECTION 107

a, b, c

Figure C-25
AXIAL GEOMETRY – CHF TEST SECTION 107

a, b, c

Figure C-26
RADIAL GEOMETRY – CHF TEST SECTION 108

a, b, c

Figure C-27
AXIAL GEOMETRY – CHF TEST SECTIONS 108 and 109

a, b, c

Figure C-28
RADIAL GEOMETRY – CHF TEST SECTION 109

a, b, c

[ ]

Figure C-29
RADIAL GEOMETRY – CHF TEST SECTION 110

a, b, c

[ ]

Figure C-30
AXIAL GEOMETRY – CHF TEST SECTION 110

a, b, c

Figure C-31
RADIAL GEOMETRY – CHF TEST SECTION 112

a, b, c

Figure C-32
AXIAL GEOMETRY – CHF TEST SECTIONS 112 and 113

a, b, c

Figure C-33
RADIAL GEOMETRY – CHF TEST SECTION 113

a, b, c

Figure C-34
RADIAL GEOMETRY – CHF TEST SECTION 83

a, b, c

Figure C-35
RADIAL GEOMETRY – CHF TEST SECTION 100

a, b, c

Figure C-36
AXIAL GEOMETRY – CHF TEST SECTION 100

a, b, c

Figure C-37
RADIAL GEOMETRY – CHF TEST SECTION 102

a, b, c

Figure C-38
AXIAL GEOMETRY – CHF TEST SECTION 102

a, b, c

[ ]

Figure C-39
RADIAL GEOMETRY – CHF TEST SECTION 103

a, b, c

Figure C-40
RADIAL GEOMETRY – CHF TEST SECTION EPRI 132

a, b, c

Figure C-41
AXIAL GEOMETRY – CHF TEST SECTION EPRI 132

a, b, c

Figure C-42
RADIAL GEOMETRY – CHF TEST SECTION EPRI 158

a, b, c

Figure C-43
AXIAL GEOMETRY – CHF TEST SECTIONS EPRI 158

a, b, c

Figure C-44
RADIAL GEOMETRY – CHF TEST SECTION EPRI 160

a, b, c

Figure C-45
AXIAL GEOMETRY – CHF TEST SECTION EPRI 160

a, b, c